



Staphylococcus aureus controls eicosanoid and specialized pro-resolving mediator production via lipoteichoic acid

Laura Miek¹ | Paul M. Jordan¹  | Kerstin Günther¹  | Simona Pace¹ |
 Timo Beyer¹ | David Kowalak¹ | Verena Hoerr² | Bettina Löffler² |
 Lorena Tuchscher² | Charles N. Serhan³ | Jana Gerstmeier¹ | Oliver Werz¹ 

¹Department of Pharmaceutical/Medicinal Chemistry, Institute of Pharmacy, Friedrich-Schiller-University Jena, Jena, Germany

²Institute of Medical Microbiology, Jena University Hospital, Jena, Germany

³Department of Anesthesiology, Perioperative and Pain Medicine, Harvard Medical School, Center for Experimental Therapeutics and Reperfusion Injury, Brigham and Women's Hospital, Boston, Massachusetts, USA

Correspondence

Oliver Werz, Department of Pharmaceutical/Medicinal Chemistry, Institute of Pharmacy, Friedrich-Schiller-University Jena, Philosophenweg 14, D-07743 Jena, Germany.
 Email: oliver.werz@uni-jena.de

Senior author: Oliver Werz.

Funding information

This work was funded by the Deutsche Forschungsgemeinschaft (DFG, German Research Foundation), Project-ID 239748522—SFB 1127 ChemBioSys—and Project-ID 316213987—SFB1278 Polytarget.

Abstract

Staphylococcus aureus causes severe infections associated with inflammation, such as sepsis or osteomyelitis. Inflammatory processes are regulated by distinct lipid mediators (LMs) but how their biosynthetic pathways are orchestrated in *S. aureus* infections is elusive. We show that *S. aureus* strikingly not only modulates pro-inflammatory, but also inflammation-resolving LM pathways in murine osteomyelitis and osteoclasts as well as in human monocyte-derived macrophages (MDMs) with different phenotype. Targeted LM metabololipidomics using ultra-performance liquid chromatography-tandem mass spectrometry revealed massive generation of LM with distinct LM signature profiles in acute and chronic phases of *S. aureus*-induced murine osteomyelitis in vivo. In human MDM, *S. aureus* elevated cyclooxygenase-2 (COX-2) and microsomal prostaglandin E₂ synthase-1 (mPGES-1), but impaired the levels of 15-lipoxygenase-1 (15-LOX-1), with respective changes in LM signature profiles initiated by these enzymes, that is, elevated PGE₂ and impaired specialized pro-resolving mediators, along with reduced M2-like phenotypic macrophage markers. The cell wall component, lipoteichoic acid (LTA), mimicked the impact of *S. aureus* elevating COX-2/mPGES-1 expression via NF- κ B and p38 MAPK signalling in MDM, while the impairment of 15-LOX-1 correlates with reduced expression of Lamtor1. In conclusion, *S. aureus* dictates LM pathways via LTA resulting in a shift from anti-inflammatory M2-like towards pro-inflammatory M1-like LM signature profiles.

KEYWORDS

inflammation, lipid mediators, macrophage

INTRODUCTION

Bacterial infections elicit acute inflammation as a protective immune reaction that helps the host to eliminate the invading microorganism, followed by active resolution of inflammation, tissue repair and regeneration [1–3].

The early inflammatory response is mediated by host-derived pro-inflammatory lipid mediators (LMs) such as prostaglandins (PG) and leukotrienes (LT), enzymatically produced via oxygenation of arachidonic acid (AA) by cyclooxygenase (COX) or 5-lipoxygenase (LOX) pathways [4] (Figure 1a). Notably, the subsequent resolution

This is an open access article under the terms of the Creative Commons Attribution-NonCommercial-NoDerivs License, which permits use and distribution in any medium, provided the original work is properly cited, the use is non-commercial and no modifications or adaptations are made.

© 2022 The Authors. *Immunology* published by John Wiley & Sons Ltd.

of inflammation is actively facilitated by a superfamily of bioactive LM, that is, the specialized pro-resolving mediators (SPMs) [3, 5] (Figure 1a). SPMs comprise lipoxins (LX), resolvins (Rv), protectins (PD) and maresins (MaR), formed by specific oxygenase pathways from AA, eicosapentaenoic acid (EPA) and docosahexaenoic acid (DHA) [6], where 15-LOXs are considered key enzymes with mainly anti-inflammatory and pro-resolving features [7–9]. SPMs are new potential therapeutics in infectious inflammation by supporting the host immune defence against bacteria and lowering antibiotic requirements [1, 10]. Notably, failure in SPM biosynthesis can result in excessive inflammatory responses and unresolved, chronic inflammation upon infection [11, 12].

Staphylococcus (S.) aureus represents the major cause for numerous life-threatening infections, such as bacteraemia, septicaemia, pneumonia, endocarditis, as well as osteomyelitis, skin and soft tissue and device-related infections [13, 14]. The interaction of *S. aureus* with the host is complex since *S. aureus* utilizes various strategies to evade the host immune response, which are likely reasons for the ineffectiveness of antibacterial treatment [15, 16]. Therefore, understanding of the cell biology of the interaction between *S. aureus* and the host, particularly phagocytic innate immune cells, is of utmost importance. We recently demonstrated that exposure of human monocyte-derived macrophages (MDMs) to *S. aureus* elicited pronounced formation of pro-inflammatory LTs and PGs from M1-MDM and marked biosynthesis of SPMs and other 15-LOX products from M2-MDM within minutes to few hours [8, 9]. In such short-term incubations (≤ 3 h), the bacteria and their virulence factors function as stimuli to activate the LM-biosynthetic pathways [8], but whether the expression of key LM pathway enzymes is affected remains unknown. Therefore, we were interested how *S. aureus* would affect the expression of LM-biosynthetic enzymes and the concomitant LM signature profiles in human MDM upon prolonged exposure (up

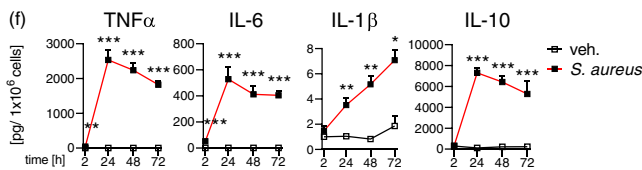
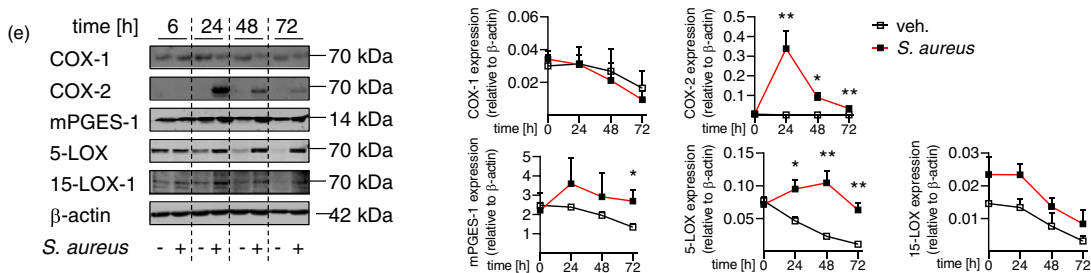
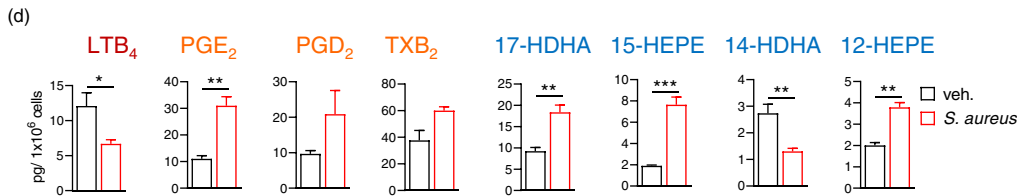
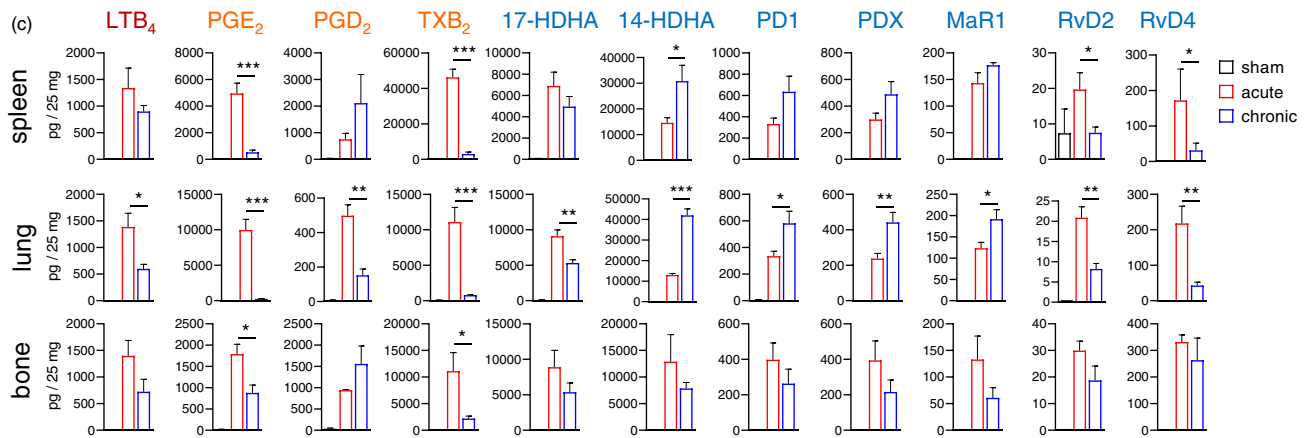
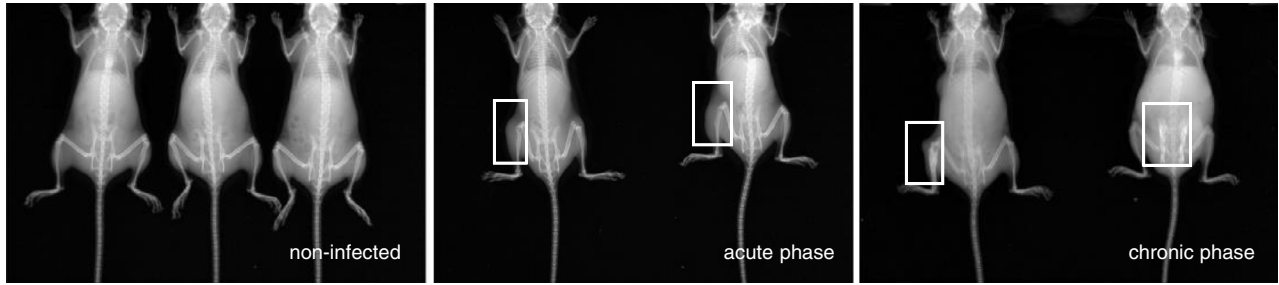
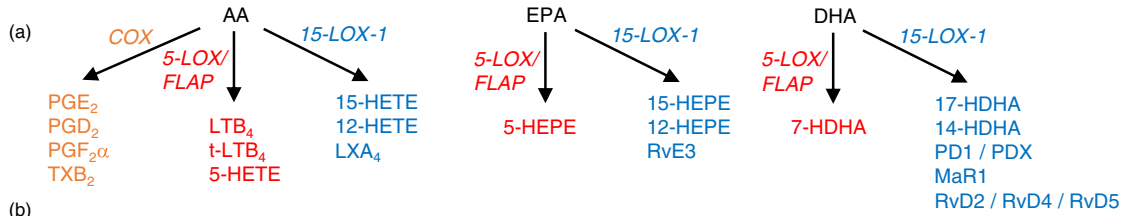
to 96 h), particularly during the acquirement of a certain macrophage phenotype. We first studied a mouse model of *S. aureus*-induced osteomyelitis in vivo and *S. aureus*-infected murine osteoclasts in vitro. Since macrophages are the main sources of precursors of osteoclasts [17], we subsequently focused on human MDM exposed to *S. aureus*. We report that in human MDM, *S. aureus*, on the one hand, causes marked induction of COX-2 and microsomal PGE₂ synthase (mPGES)-1 protein expression, while suppressing IL-4-induced 15-LOX-1 protein levels during macrophage polarization. These actions of *S. aureus* in human MDM were mimicked by lipoteichoic acid (LTA), a major cell wall component of Gram-positive bacteria [18, 19], and lead to a shift from pro-resolving towards pro-inflammatory LM.

RESULTS

Formation of lipid mediators in *S. aureus*-induced murine osteomyelitis in vivo

Osteomyelitis represents a bone infection associated with destruction of bone tissue, which is prevalently caused by *S. aureus* [20, 21] and frequently develops a chronic course with relapsing infection despite proper antimicrobial treatment [22, 23]. We studied the LM signature profiles by targeted LM metabololipidomics using ultra-performance liquid chromatography-tandem mass spectrometry (UPLC-MS/MS) in mouse models of acute (1 week) and chronic (6 weeks) osteomyelitis in vivo, induced upon *i.v.* infection with *S. aureus* [24]. X-ray images showed swelling and initial bone destruction during the acute phase (1 week), with marked swelling and bone remodelling during the chronic phase (6 weeks; Figure 1b). LMs were analysed not only in the bone, but also in spleen and lung. The amounts of many specific LM were strikingly increased

FIGURE 1 LM profiles in a mouse model of acute and chronic osteomyelitis in vivo and in murine osteoclasts. (a) Schematic representation of the investigated LM-biosynthetic pathways involving COX, 5-LOX or 15-LOX-1 leading to respective LM. (b–c) Female mice received *S. aureus* (10^6 CFU/ 200 μ l) by *i.v.* injection. (b) Bone destruction was monitored by X-ray imaging both in the acute phase (1 week) and chronic phase (6 weeks) of the infection. (c) Biosynthesized LMs were isolated from spleen, lung and bone and analysed by UPLC-MS/MS. Bar charts of selected LM are shown as pg/25 mg tissue. Results are given as means + SEM; $n = 3$ –5; * $p < 0.05$; ** $p < 0.01$; *** $p < 0.001$, acute phase versus chronic phase. (d–f) Murine osteoclasts were exposed to *S. aureus* for 2 h, treated with lysostaphin for 30 min, and further cultivated for the indicated times. (D) Both vehicle- and *S. aureus*-treated cells were stimulated with SACM (0.5%) in PBS plus 1 mM CaCl₂ for 60 min. Osteoclasts were stimulated with SACM (0.5%) in PBS plus 1 mM CaCl₂ for 60 min. LMs in the supernatants were analysed by UPLC-MS/MS. Bar charts of selected LM are shown as pg/10⁶ cells. Results are given as means + SEM at 72 h; $n = 3$; * $p < 0.05$; ** $p < 0.01$; *** $p < 0.001$, *S. aureus* versus vehicle. (e) Cells were immunoblotted for COX-1, COX-2, mPGES-1, 5-LOX and 15-LOX-1, and normalized to β -actin for densitometric analysis. Exemplary results (left panel) and densitometric analysis (right panel) are shown; data are shown as means + SEM; $n = 3$; * $p < 0.05$; ** $p < 0.01$ *S. aureus* versus vehicle. (f) Cytokines released from osteoclasts, shown as pg/10⁶ cells. Results are given as means + SEM; $n = 3$; * $p < 0.05$; ** $p < 0.01$; *** $p < 0.001$, *S. aureus* versus vehicle. Data were log-transformed for statistical analysis, unpaired Student's *t*-test (c–f). See also Table S1 and Table S2



in infected mice in the acute phase vs. sham animals, irrespective of the tissue type (Figure 1c and Table S1). During the chronic phase, 5-LOX- and COX-derived products were decreased in all three tissues vs. the acute phase, except PGD₂ in bone and spleen that was further elevated. Of interest, among SPMs in spleen and lung, PD1, PDX, MaR1 and 14-HDHA increased during the chronic phase, while RvD2, RvD4, RvE3, LXA₄ and other 12/15-LOX-derived products were diminished (Figure 1a, c and Table S1). In bone, none of the SPMs were elevated in the chronic vs. the acute phase.

To study the modulation of LM pathways by *S. aureus* in an osteomyelitis-relevant model on the cellular level, we exposed murine osteoclasts to *S. aureus*. To avoid osteoclast cell death due to unhindered and excessive bacterial growth, we exploited a lysostaphin protection assay [25, 26]. Thus, osteoclasts were exposed to *S. aureus* at a multiplicity of infection (MOI) of 10 for only 2 h, extracellular bacteria were then eliminated by lysostaphin and osteoclasts were further cultivated for up to 72 h to impact expression of LM-biosynthetic enzymes. To fully activate these enzymes and thus to elicit LM formation, the osteoclasts were treated with *S. aureus*-conditioned medium (SACM) for 1 h as suitable stimulus, as reported before [8]. In the absence of *S. aureus*, osteoclasts exposed to SACM produced several LM, including pro-inflammatory COX- and 5-LOX-derived eicosanoids as well as 12/15-LOX products and other monohydroxy-containing products, but SPMs were not generated (Figure 1d and Table S2). Pre-exposure to *S. aureus* decreased the generation of 5-LOX-derived LM after 24–72 h, but elevated formation of prostanoids (PGE₂, PGD₂, PGF_{2α}, TXB₂) after 24 h that subsequently declined (Figure 1d and Table S2). The mouse 12/15-LOX-derived LMs were inconsistently modulated; for instance, 17-HDHA, 15-HEPE and 12-HEPE levels were increased, but 14-HDHA formation was impaired (Figure 1d and Table S2). We then assessed whether the exposure to *S. aureus* impacts the protein levels of LM-biosynthetic enzymes in murine osteoclasts. COX-2 and mPGES-1 levels were increased and peaked 24 h after exposure to *S. aureus* with subsequent moderate temporal decline (Figure 1e). Surprisingly, 5-LOX protein levels were elevated by *S. aureus*, particularly at later time points (48 and 72 h), whereas 15-LOX levels were not affected (Figure 1e). Besides LM, we also analysed cytokines that were shown to be secreted by osteoclasts upon *S. aureus* exposure [27]. The release of tumour necrosis factor (TNF)α, interleukin (IL)-6, IL-1β and IL-10 significantly increased upon *S. aureus* exposure, although the absolute amounts of these cytokines were low, except for IL-10 (Figure 1f).

***S. aureus* impacts production of cytokines and lipid mediators in human MDM**

To explore whether the modulation of LM pathways by *S. aureus* is also a common pattern in other cell types and other species, particularly in human innate immune cells, we investigated human MDM that like osteoclasts derive from monocytes but possess high capacities to produce a large panel of LM in response to *S. aureus* exotoxins, depending on their phenotype [8, 9]. Macrophages are considered as precursors of osteoclasts [17] as they can switch from an inflammatory phenotype towards differentiation into osteoclasts [28]. Human MDMs were exposed to *S. aureus* at a low MOI of 2 in parallel to polarization towards M1-like cells using interferon-γ (IFN-γ; designated as M_{IFN-γ}) and towards M2-like MDM using IL-4 (M_{IL-4}) or devoid of polarization (M₀). After 2 h of infection, external bacteria were eliminated by lysostaphin, and MDMs were cultured for up to 96 h (Figure 2a). Analysis of intracellular bacterial loads showed that approximately 10⁶ colony forming units (CFU) remained per 10⁶ MDM (M₀, M_{IFN-γ} and M_{IL-4}) up to 6 h after lysostaphin treatment, which declined to approximately 10³ CFU per 10⁶ MDM at 48 h and bacteria were completely cleared after 96 h post-infection, except in M_{IL-4} where some intracellular bacteria still remained (Figure 2b). Regardless of the MDM phenotype, *S. aureus* caused substantial release of the pro-inflammatory cytokines IL-1β, TNFα and IL-6 with maximal effects at 6, 24 and 96 h post-*S. aureus* infection, respectively, while anti-inflammatory IL-10 was hardly affected (Figure 2c).

96 h upon *S. aureus* infection, defined alterations in SACM-induced generation of bioactive LM, largely independent of the MDM phenotype, were evident (Table 1 and Figure 2d). Thus, the formation of 5-LOX-derived LM (e.g. LTB₄) declined, while formation of COX-derived PGE₂ strongly increased due to precedent *S. aureus* exposure (Table 1 and Figure 2d). Also, PGD₂ was elevated in M₀ and M_{IFN-γ} by *S. aureus*, but decreased in M_{IL-4}, and other COX-derived LM like PGF_{2α} or TXB₂ were either unaffected or impaired, particularly in M_{IL-4} (Table 1). Moreover, the robust formation of SPMs and other prominent 15-LOX-derived products (e.g. 17-HDHA, 15-HETE, 15-HEPE, 12-HETE, 5,15-diHETE) in M_{IL-4} was reduced upon exposure to *S. aureus*, but also in M₀ and M_{IFN-γ} (Table 1 and Figure 2d). The levels of the substrates AA, DHA and EPA were slightly elevated from the bacterial challenge in M₀ and M_{IFN-γ}, but more prominent in the M_{IL-4} (Table 1). Together, the exposure of MDM impairs 5-LOX- and 15-LOX-derived LM formation, but potently increases the formation of PGE₂ in all MDM phenotypes, with relatively minor or no elevations of other COX-derived prostanoids.

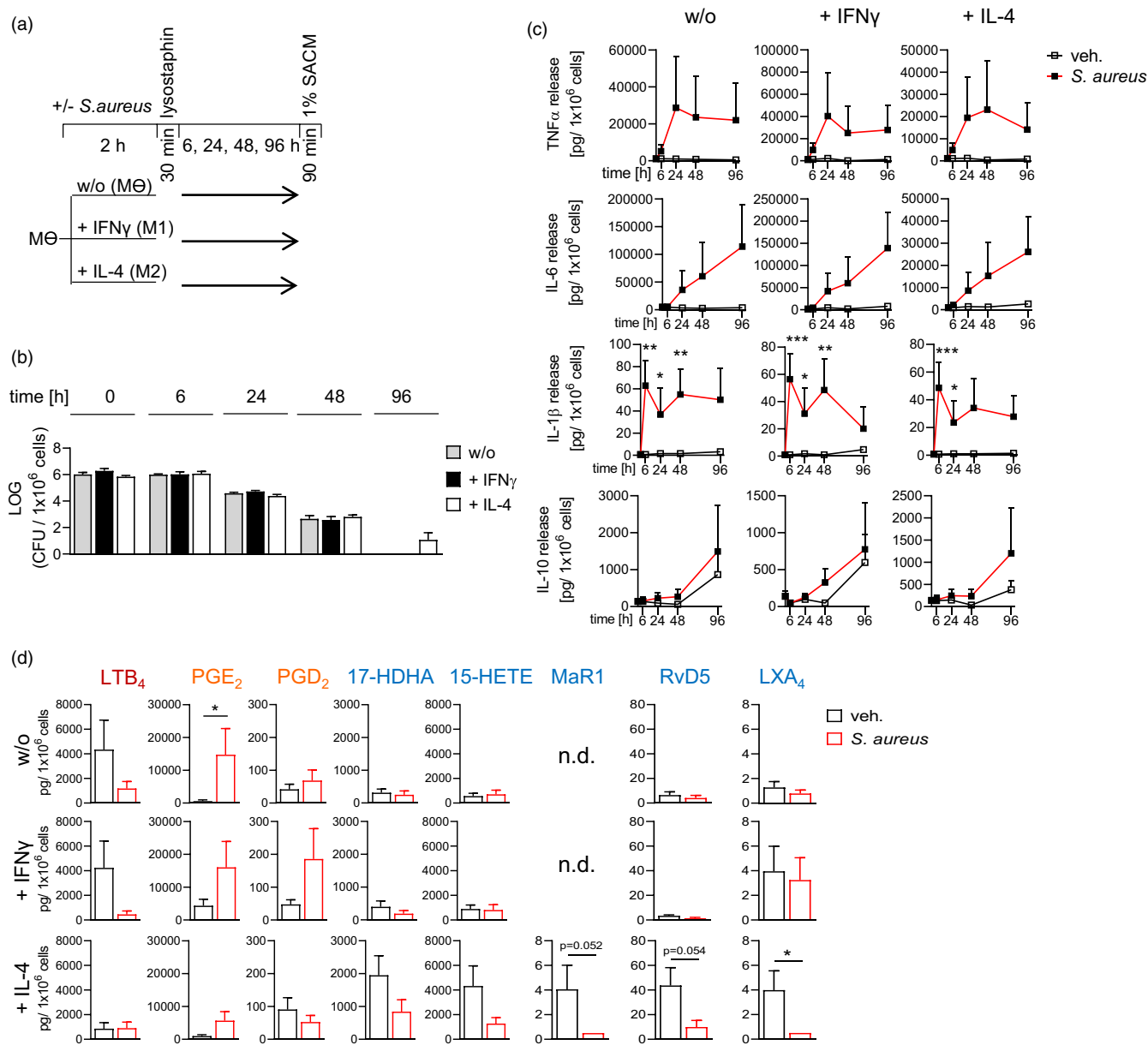


FIGURE 2 *S. aureus* dictates formation of cytokines and lipid mediators in human MDM. (a–d) M₀ were treated with IFN- γ , IL-4 or vehicle in the absence or presence of *S. aureus* 6850 for 2 h, treated with lysostaphin for 30 min and further grown with IFN- γ , IL-4 or vehicle (w/o) for the indicated times. (a) Schematic presentation of the experimental setup. (b) Cells were detached, lysed and intracellular bacterial loads were determined. Data are means + SEM; $n = 3$ separate donors. (c) Cytokines released by macrophages, shown as pg/ 10^6 cells. Results are given as means + SEM; $n = 3$ –4 separate donors; * $p < 0.05$; ** $p < 0.01$; *** $p < 0.001$, *S. aureus* versus vehicle. (d) Both vehicle- and *S. aureus*-treated cells were stimulated with SACM (1%) in PBS plus 1 mM CaCl₂ for 90 min. LMs in the supernatants were analysed by UPLC-MS/MS. Data were normalized to the protein content of macrophages ($\mu\text{g}/\text{ml}$); vehicle-treated M₀, M_{IFN- γ} or M_{IL-4} for 6 h were used for normalization (100%). Bar charts of selected LM are shown as pg/ 10^6 cells. Results are means + SEM at 96 h; $n = 4$ –5 separate donors; * $p < 0.05$, *S. aureus* versus vehicle. Data were log-transformed for statistical analysis, unpaired Student's *t*-test (c, d)

S. aureus differentially modulates lipid mediator-biosynthetic enzyme expression

The capacities to produce LM mainly depend not only on the levels of free PUFA, but also on the amounts of LM-biosynthetic enzymes in the cell. Thus, we next investigated whether the exposure of MDM to *S. aureus*

would impact the protein levels of LM-biosynthetic enzymes. While the levels of the constitutively expressed COX-1 were unaffected, those of inducible COX-2 were significantly increased in all three MDM types 6 h post-infection with *S. aureus* and remained high in M₀ and M_{IFN- γ} up to 96 h, while they declined after 24 up to 96 h in M_{IL-4} (Figure 3a and S1). Besides COX-2, also mPGES-1

TABLE 1 LM signature profiles of MDM exposed to *S. aureus*^a

Time [h]	w/o			+ IFN- γ			+ IL-4						
	6			96			96						
	Veh.	<i>S. aureus</i>	-Fold	Veh.	<i>S. aureus</i>	-fold	Veh.	<i>S. aureus</i>	-Fold				
5-LOX/FLAP	5-HEPE	1265 ± 411	665 ± 171	0.5	247 ± 105	288 ± 142	1.2	682 ± 282	244 ± 116	0.4	182 ± 84	202 ± 100	1.1
	t-LTB ₄	1186 ± 302	646 ± 284	0.5	1212 ± 608	495 ± 272	0.4	1628 ± 693	578 ± 348	0.4	428 ± 207	365 ± 206	0.9
	LTB ₄	2281 ± 875	990 ± 239	0.4	4342 ± 2397	1181 ± 564	0.3	4236 ± 2173	456 ± 275	0.1	857 ± 495	904 ± 494	1.1
	5-HETE	7442 ± 1932	3899 ± 966	0.5	4944 ± 2007	798 ± 387	0.2	6186 ± 2310	1608 ± 846	0.3	1489 ± 655	1465 ± 833	1.0
COX	PGE ₂	552 ± 267	1044 ± 546	1.9	601 ± 372	14734 ± 7966	25	4346 ± 1973	16043 ± 7862	4	982 ± 410	5660 ± 2745	6
	PGD ₂	154 ± 79	411 ± 234	3	42 ± 16	68 ± 32	1.6	47 ± 14	186 ± 92	4	91 ± 36	53 ± 20	0.6
	PGF _{2α}	421 ± 159	322 ± 168	0.8	211 ± 69	233 ± 103	1.1	190 ± 47	279 ± 134	1.5	183 ± 34	163 ± 63	0.9
	TXB ₂	20914 ± 8007	23254 ± 8024	1.1	7011 ± 1866	4286 ± 1755	0.6	6010 ± 944	4606 ± 1977	0.8	14762 ± 5509	4557 ± 1906	0.3
Mono-/dihydroxylated	17-HDHA	77 ± 17	152 ± 33	2	314 ± 110	250 ± 117	0.8	398 ± 179	190 ± 95	0.5	1950 ± 594	840 ± 364	0.4
	15-HEPE	15 ± 2	30 ± 9	2	26 ± 7	39 ± 14	1.5	40 ± 18	18 ± 4	0.4	230 ± 85	97 ± 33	0.4
	15-HETE	705 ± 177	798 ± 160	1.1	565 ± 227	708 ± 342	1.3	892 ± 324	805 ± 434	0.9	4325 ± 1639	1272 ± 487	0.3
	14-HDHA	9 ± 0.3	24 ± 4	3	11 ± 6	20 ± 5	1.7	11 ± 4	20 ± 7	1.7	71 ± 22	27 ± 7	0.4
Bioactive SPM	12-HEPE	15 ± 5	16 ± 4	1.1	2 ± 0.3	9 ± 1.5	4	4 ± 1.3	7 ± 2	1.8	16 ± 6	8 ± 1.4	0.5
	12-HETE	83 ± 23	96 ± 22	1.2	35 ± 14	28 ± 5	0.8	36 ± 11	25 ± 6	0.7	106 ± 45	32 ± 6	0.3
	5,15-diHETE	270 ± 108	275 ± 111	1.0	171 ± 82	86 ± 36	0.5	114 ± 27	59 ± 25	0.5	702 ± 398	186 ± 91	0.3
	18-HEPE	10 ± 0.8	16 ± 4.0	1.6	10 ± 3	20 ± 4	2	11 ± 3	18 ± 4	1.7	8 ± 1.5	19 ± 2	2
Bioactive SPM	7-HDHA	91 ± 26	105 ± 34	1.2	55 ± 19	33 ± 12	0.6	48 ± 19	35 ± 16	0.7	26 ± 7	28 ± 10	1.1
	4-HDHA	15 ± 0.9	18 ± 1.9	1.2	13 ± 4	20 ± 4	1.5	15 ± 4	18 ± 5	1.2	6 ± 1.5	16 ± 4	2
	PD1	0.7 ± 0.2	1.8 ± 0.4	2	1.4 ± 0.3	4 ± 0.9	3	1.9 ± 0.6	3 ± 1.0	1.5	5 ± 1.6	8 ± 4	1.6
	AT-PDI	1.0 ± 0.4	2 ± 0.5	2	3 ± 1.6	4 ± 1.2	1.3	1.7 ± 0.5	4 ± 1.3	2	6 ± 2	8 ± 4	1.5
	PDX	0.5 ± 0.0	0.9 ± 0.2	1.7	1.0 ± 0.2	1.1 ± 0.3	1.2	0.6 ± 0.1	0.9 ± 0.2	1.4	1.0 ± 0.1	0.9 ± 0.1	0.9
	Mar1	0.5 ± 0.0	0.5 ± 0.0	1.0	0.5 ± 0.0	0.5 ± 0.0	1.0	0.5 ± 0.0	0.5 ± 0.0	1.0	4 ± 2	0.5 ± 0.0	0.1
	RvD5	10 ± 4	7 ± 2	0.7	6 ± 3	4 ± 2	0.6	3 ± 0.8	1.4 ± 0.7	0.4	44 ± 15	10 ± 5	0.2
	LXA ₄	4 ± 1.9	4 ± 2	0.9	1.3 ± 0.5	0.8 ± 0.3	0.6	4 ± 2	3 ± 1.8	0.8	4 ± 1.6	0.5 ± 0.0	0.1
	AT-LXA ₄	4 ± 2	6 ± 2	1.4	0.5 ± 0.0	0.5 ± 0.0	1.0	0.5 ± 0.0	0.5 ± 0.0	1.0	1.4 ± 0.9	0.5 ± 0.0	0.4
	AA	324 580 ± 66 405	418 376 ± 58 990	1.3	365 878 ± 69 273	510 197 ± 142 377	1.4	396 557 ± 90 389	450 136 ± 105 927	1.1	165 756 ± 44 807	413 654 ± 72 520	2
EPA		85 254 ± 12 486	114 624 ± 16 499	1.3	55 240 ± 10 296	130 340 ± 39 755	2	74 598 ± 25 537	114 094 ± 34 871	1.5	18 072 ± 4205	98 991 ± 22 935	5
	DHA	38 207 ± 11 379	60 628 ± 12 197	1.6	67 661 ± 3914	104 379 ± 30 435	1.5	62 553 ± 14 196	85 211 ± 20 907	1.4	22 522 ± 5595	74 942 ± 13 664	3

^aM₀ were treated with IFN- γ or IL-4 in the absence or presence of *S. aureus* 6850 for 2 h, treated with lysostaphin for 30 min and further grown with IFN- γ , IL-4 or vehicle (w/o) for 6 or 96 h, as indicated. Both vehicle- and *S. aureus*-treated cells were then stimulated with SACM (1%) in PBS plus 1 mM CaCl₂ for 90 min. LMs in the supernatants were analysed by UPLC-MS/MS. Data were normalized to the protein content of macrophages ($\mu\text{g/ml}$); vehicle-treated M₀, M_{IFN- γ} or M_{IL-4} for 6 h were used for normalization (100%). Data are presented as pg/10⁶ cells and LM as -fold increase in each LM against vehicle-treated cells after 96 h; n = 4–5 separate donors.

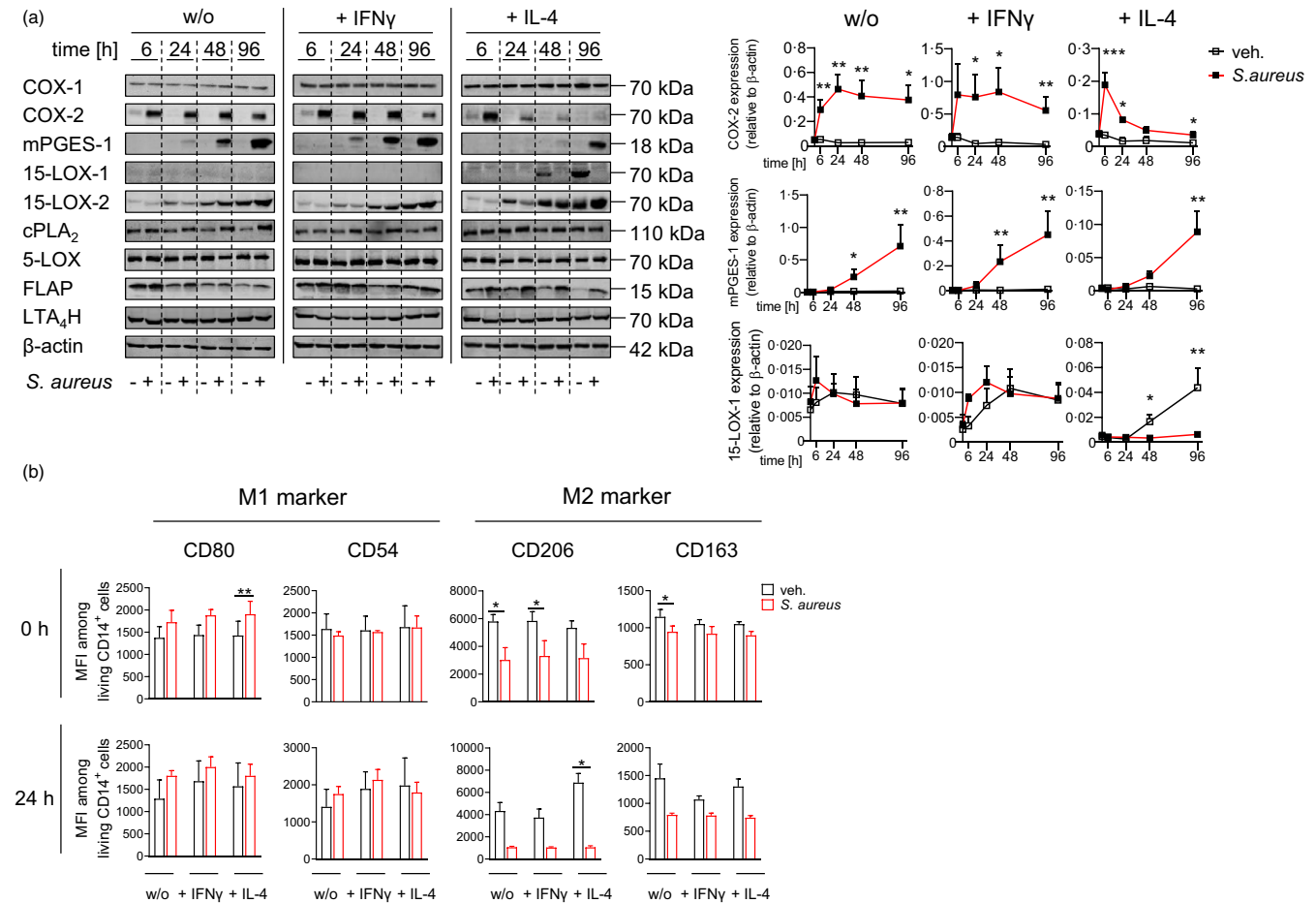


FIGURE 3 Modulation of the levels of LM-biosynthetic enzymes and surface markers in human MDM by *S. aureus*. (a, b) M_0 were treated with IFN- γ , IL-4 or vehicle in the absence or presence of *S. aureus* 6850 for 2 h, treated with lysostaphin for 30 min and further grown with IFN- γ , IL-4 or vehicle (w/o) for the indicated times. (a) Cells were harvested and immunoblotted for the indicated proteins and normalized to β -actin for densitometric analysis. Exemplary results (left panel) and densitometric analysis (right panel) are shown. Data are means + SEM; $n = 4-7$ separate donors; * $p < 0.05$; ** $p < 0.01$; *** $p < 0.001$, *S. aureus* versus vehicle. Data were log-transformed for statistical analysis, unpaired Student's *t*-test. (b) Expression of M1 markers CD80, CD54 and M2 markers CD206, CD163 was measured by flow cytometry. Data are presented as mean fluorescence intensity of the respective markers among living CD14⁺ cells. Results are given as means + SEM; $n = 3$ separate donors; * $p < 0.05$, ** $p < 0.01$, *S. aureus* versus vehicle. For statistical analysis, paired Student's *t*-test was used. See also Figures S1–S3

expression was strongly increased in M_0 and $M_{\text{IFN-}\gamma}$ upon *S. aureus* infection for ≥ 48 h and, somewhat delayed also in $M_{\text{IL-4}}$. In contrast, 15-LOX-1, which is induced during M2 polarization but not in other MDM phenotypes, was strongly suppressed by *S. aureus* (Figure 3a), explaining why 12/15-LOX products were impaired despite elevated PUFA levels (Table 1). Note that the protein levels of other LM-biosynthetic enzymes, for example, 15-LOX-2, cytosolic phospholipase A₂ (cPLA₂), 5-LOX, 5-LOX-activating protein (FLAP) and LTA₄ hydrolase (LTA₄H), remained unaffected or were only slightly but not significantly altered (e.g. COX-1 and 5-LOX in $M_{\text{IL-4}}$ at 96 h) (Figures 3a and S1), highlighting COX-2, mPGES-1 and 15-LOX-1 as highly susceptible proteins for modulation by *S. aureus*.

To study how *S. aureus* affects the MDM phenotype during polarization, the expression of characteristic M1/M2 surface

markers was analysed by flow cytometry. Exposure to *S. aureus* caused a slight increase in the M1 markers CD80 and CD54, while it caused a strong decrease in the M2 markers CD206 and CD163 in all three MDM subtypes, suggesting that *S. aureus* shifts MDM from M2-like towards an M1-like phenotype (Figures 3b and S2). Note that cell viability of the MDM was not markedly affected up to 96 h by *S. aureus* exposure (for 2 h and subsequent extracellular bacterial killing with lysostaphin; Figure S3a).

Attenuated *S. aureus* accomplish the MDM-modulatory effects of vital bacteria

Staphylococcus aureus may impact cytokines and LM-biosynthetic pathways in MDM in two different ways:

(i) the initial exposure of MDM might be sufficient to trigger the response and (ii) the permanent presence of intracellular live bacteria might be causative. When *S. aureus* was attenuated by heat inactivation prior to addition to MDM, the release of cytokines tended to increase (Figure S4), as with vital *S. aureus*, although with a lower magnitude. Also, the strong elevation of COX-derived PGE₂ and PGD₂ by M₀ and M_{IFN-γ} was obvious for attenuated *S. aureus* (Figure 4a and Table S3). In contrast, 5-LOX-derived LMs were rather increased (Figure 4a and Table S3), indicating that suppression of 5-LOX product formation requires vital *S. aureus*. The production of 15-LOX-derived LM and the levels of AA, DHA and EPA remained largely unaffected in response to attenuated *S. aureus* in all MDM phenotypes.

However, 15-LOX-derived SPMs in M_{IL-4} were reduced upon incubation with attenuated *S. aureus* as compared to vital bacteria (Figure 4a and Table S3).

Modulation of protein levels of LM-biosynthetic enzymes in MDM by attenuated *S. aureus* was similar as for vital *S. aureus* with most prominent effects at 96 h. Thus, COX-2 and mPGES-1 levels were increased, whereas 15-LOX-1 protein amounts were impaired, and expression of 15-LOX-2, cPLA₂, 5-LOX, FLAP and LTA₄H was hardly affected (Figures 4b and S5). Conclusively, the modulatory effects of *S. aureus* on MDM are at least partially caused by bacterial component(s), present in vital and attenuated *S. aureus*. Like for vital *S. aureus*, the viability of MDM was not markedly affected by exposure to attenuated bacteria (Figure S3b).

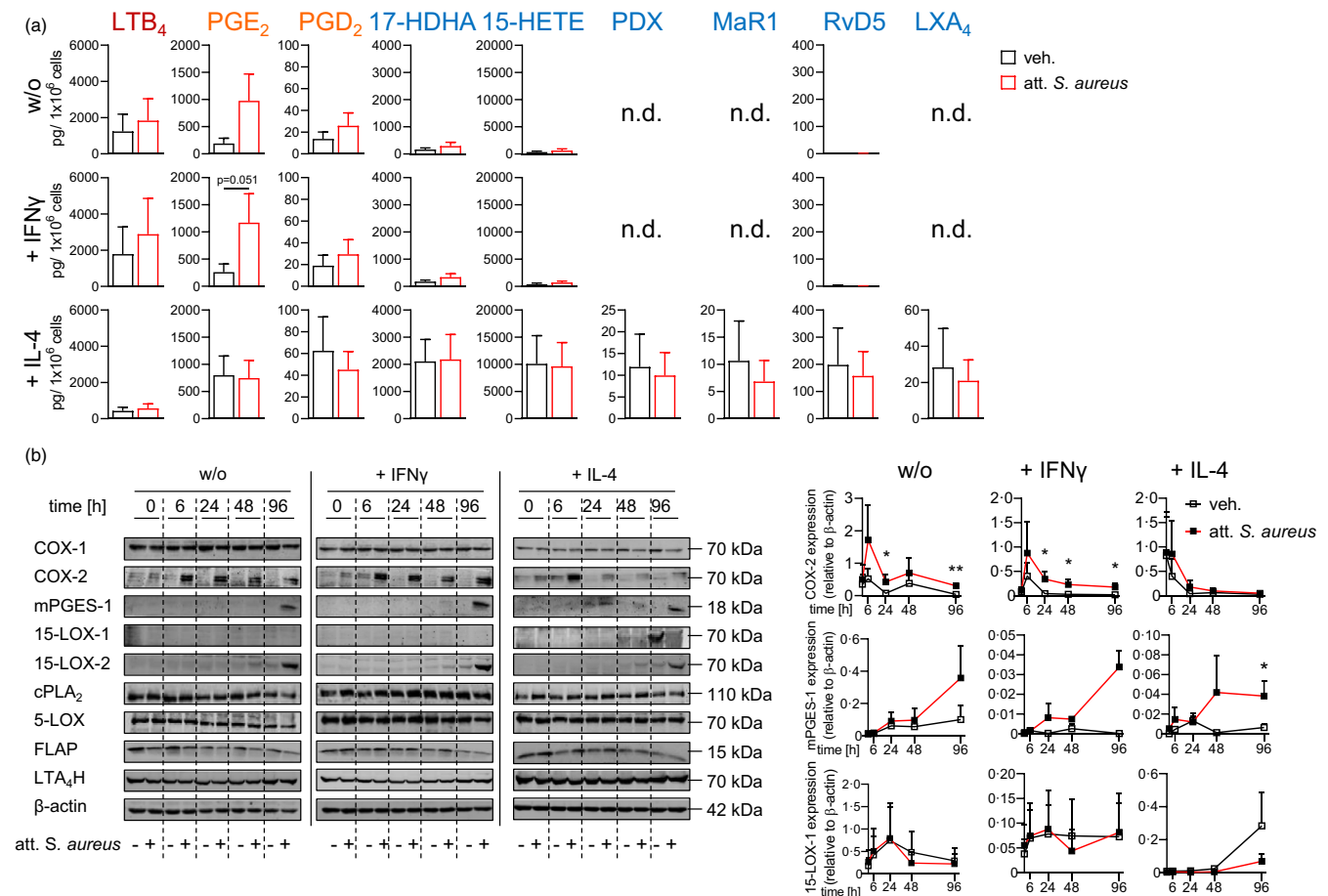


FIGURE 4 Attenuated *S. aureus* accomplish the MDM-modulatory effects of vital *S. aureus*. (a, b) M₀ were treated with IFN-γ, IL-4 or vehicle in the absence or presence of attenuated *S. aureus* (treatment at 95°C for 10 min) for 2 h, treated with lysostaphin for 30 min and further grown with IFN-γ, IL-4 or vehicle (w/o) for the indicated times. (a) Both vehicle- and attenuated *S. aureus*-treated cells were stimulated with SACM (1%) in PBS plus 1 mM CaCl₂ for 90 min. LMs in the supernatants were analysed by UPLC-MS/MS. Data were normalized to the protein content of macrophages (μg/ml); vehicle-treated M₀, M_{IFN-γ} or M_{IL-4} for 6 h were used for normalization (100%). Bar charts of selected LM are shown as pg/10⁶ cells. Results are means + SEM at timepoint 96 h; n = 3–5 separate donors; attenuated *S. aureus* versus vehicle. (b) Cells were immunoblotted for the indicated proteins and normalized to β-actin for densitometric analysis. Exemplary results (left panel) and densitometric analysis (right panel) are shown. Data are shown as means + SEM; n = 3–7 separate donors; *p < 0.05; **p < 0.01, attenuated *S. aureus* versus vehicle. Data were log-transformed for statistical analysis; unpaired Student's *t*-test (a, b). See also Figures S4 and S5 and Table S3

LTA mimics *S. aureus*-induced modulation of LM biosynthesis

LTA, a cell wall component of Gram-positive bacteria, such as *S. aureus* binds to toll-like receptor (TLR)-2 [19, 29] and induces inflammatory responses such as secretion of TNF α , IL-6, IL-1 β and IL-10 from various leukocytes, and increased COX-2 expression [30]. We hypothesized that LTA, which is released spontaneously into the culture medium during growth of *S. aureus* [18], may represent the active principle of *S. aureus*-induced modulation of LM-biosynthetic pathways. Release of LTA from intact *S. aureus* was substantial after 4-h culture with marked decline after 24 h, whereas LTA was hardly present in the corresponding SACM after 4 h, but strongly elevated after 24 h (Figure 5a). The amount of LTA released from intact *S. aureus* at MOI 2 was estimated at approximately 0.3–0.5 μ g LTA per ml from the WB data. We therefore performed subsequent experiments with 1 μ g/ml recombinant LTA. Treatment of MDM with 1 μ g/ml LTA during polarization impaired cell viability, but still more than 60% of the cells were viable after 96 h (Figure S3c). The release of cytokines by MDM was increased upon LTA addition, being rapid for TNF α and IL-6 (i.e. maximum at 6–24 h) and somewhat delayed for IL-1 β and IL-10 (maximum at 48 h) (Figure 5b). In contrast to *S. aureus*, 5-LOX product formation after 96 h was increased in LTA-treated MDM, especially in M_{IL-4} (Figure 5c). Note that LTA after 96 h significantly elevated PGE₂ biosynthesis in M₀ and M_{IFN- γ} , but less in M_{IL-4}, while PGD₂, PGF_{2 α} and TXB₂ were not affected or decreased in all subtypes (Figure 5c and Table S4). Formation of 12/15-LOX-derived LM (e.g. 17-HDHA, 15-HETE) including SPM as well as the release of AA, EPA and DHA was hardly altered or slightly elevated by LTA (Figure 5c and Table S4). In agreement with marked PGE₂ formation, LTA increased mPGES-1 protein levels in M₀ and M_{IFN- γ} , but not in M_{IL-4}, at 24, 48 and 96 h (Figure 5d). COX-2 protein levels were strongly elevated by LTA after 6 h but declined afterwards in all MDM phenotypes (Figure 5d). In analogy to *S. aureus*, LTA prevented IL-4-induced 15-LOX-1 expression in M_{IL-4} (Figure 5d). Note that 15-LOX-derived LMs including SPM were only hardly diminished by LTA in M_{IL-4}, possibly because 15-LOX-2 was still expressed (Figure S6) that accomplished 15-LOX product formation. Because LTA acts as TLR-2 agonist [19, 29], we studied the involvement of the TLR-2 in LM pathways induced by LTA. TLR-2 (CD282) expression in M₀ was confirmed by flow cytometry and was hardly affected by exposure to *S. aureus* up to 96 h (Figure S7). To determine the role of TLR-2 in LTA-elevated LM formation, we employed the TLR-2-specific inhibitor MMG-11 (Biozol, Eching, Germany). Only formation of those LM that were increased by LTA

6 h after exposure, in particular COX products, was impaired by MMG-11 but not basal LM production of, for example, 17-HDHA or 7-HDHA (Figure 5e, Table S5), indicating the requirement of TLR-2 for LTA-triggered LM biosynthesis. Together, LTA essentially mimicked the effects of *S. aureus* on LM pathways: it strongly enhanced COX-2 and mPGES-1 expression along with marked PGE₂ formation in M₀ and M_{IFN- γ} but suppressed 15-LOX-1 protein levels in M_{IL-4}.

Elevation of COX-2 and mPGES-1 protein by LTA involves NF- κ B and p38 MAPK while downregulation of 15-LOX-1 protein correlates with Lamtor1 expression

Next, we studied whether NF- κ B, p38 MAPK, JNK and ERK-1/2 that typically act upstream of induction of COX-2 expression [31–34] play a role in LTA-induced elevation of COX-2 protein levels. LTA enhanced the phosphorylation of NF- κ B, p38 MAPK and JNK in both M_{IFN- γ} and M_{IL-4} with a peak at 60 min upon exposure (Figure 6a). The levels of phosphorylated ERK-1/2 were not affected by LTA (Figure S8). To assess the requirement of NF- κ B, p38 MAPK and JNK signalling in LTA-induced elevation of COX-2 protein levels, we employed parthenolide, skepinone-L and SP600125 to block the respective pathway. The inhibitors had only weak effects on MDM viability after 6-h incubation (Figure S9a). Blocking NF- κ B with parthenolide strongly impaired LTA-induced COX-2 expression in M_{IFN- γ} and M_{IL-4}. Inhibition of p38 MAPK by skepinone-L was less effective and interference with JNK by SP600125 hardly reverted COX-2 expression (Figure 6b). Since the functionally coupled COX-2 and mPGES-1 are often co-induced by various stimuli, we speculated that NF- κ B and p38 MAPK may regulate also LTA-induced mPGES-1 expression. Because LTA-evoked mPGES-1 expression was delayed versus COX-2 and largely absent in M_{IL-4}, we treated only M_{IFN- γ} with the inhibitors, and in this case for 48 h. In analogy to COX-2, blockade of NF- κ B and p38 MAPK abrogated LTA-induced elevation of mPGES-1 levels while inhibition of JNK was less effective (Figure 6c). Also, after 48 h, cell viability was not substantially affected by the inhibitors (Figure S9b). Together, these results suggest that LTA elevates COX-2 and mPGES-1 expression via NF- κ B and, to a minor extent, also via p38 MAPK.

Finally, we investigated which of the multiple signalling pathways that regulate 15-LOX-1 expression [35] (Figure S10a) might be affected by *S. aureus* and LTA in M_{IL-4} leading to reduced 15-LOX-1 protein levels. Addition of celecoxib to *S. aureus*-treated M_{IL-4} to block the COX-2-mediated increase in PGE₂ failed to

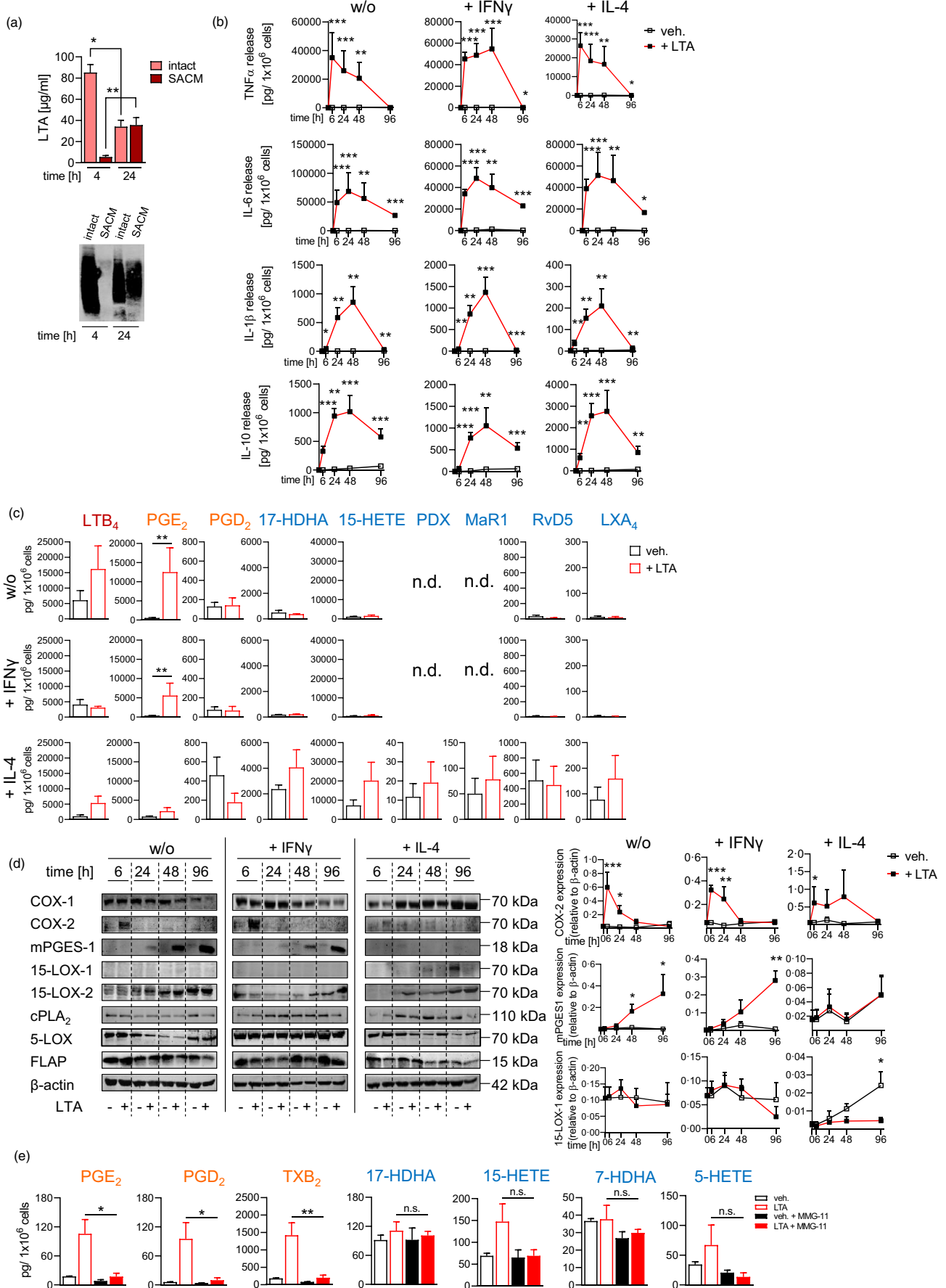


FIGURE 5 Effects of LTA from *S. aureus* on LM pathways in human MDM. (a–d) M₀ were treated with IFN- γ , IL-4 or vehicle (w/o) in the absence or presence of 1 $\mu\text{g/ml}$ LTA for the indicated times. (a) LTA in intact *S. aureus* and in SACM was immunoblotted. Densitometric analysis (upper panel) and exemplary blot (lower panel) are shown. Results are means + SEM; $n = 3$ –4 separate bacteria cultures; * $p < 0.05$, ** $p < 0.01$, 4 h versus 24 h. (b) Cytokines released by MDM, shown as $\text{pg}/10^6$ cells. Results are means + SEM; $n = 3$ separate donors; * $p < 0.05$; ** $p < 0.01$; *** $p < 0.001$, LTA versus vehicle. (c) Both vehicle- and LTA-treated cells were stimulated with SACM (1%) in PBS plus 1 mM CaCl_2 for 90 min. LMs in the supernatants were analysed by UPLC-MS/MS. Data were normalized to the protein content of macrophages ($\mu\text{g/ml}$); vehicle-treated M₀, M_{IFN- γ} or M_{IL-4} grown for 6 h were used for normalization (100%). Bar charts of selected LM are shown as $\text{pg}/10^6$ cells. Results are means + SEM at 96 h; $n = 4$ separate donors; ** $p < 0.01$, LTA versus vehicle. (d) Cells were immunoblotted for the indicated proteins and normalized to β -actin for densitometric analysis. Exemplary results (left panel) and densitometric analysis (right panel) are shown. Data are means + SEM; $n = 3$ –8 separate donors; * $p < 0.05$; ** $p < 0.01$; *** $p < 0.001$, LTA versus vehicle. Data in a–d were log-transformed for statistical analysis, unpaired Student's *t*-test. (e) M₀ were treated with 25 μM MMG-11 or vehicle control in the absence or presence of 1 $\mu\text{g/ml}$ LTA for 6 h and LM were analysed in the supernatants by UPLC-MS/MS. Bar charts of selected LM are shown as $\text{pg}/10^6$ cells. Results are means + SEM; $n = 3$ separate donors; statistical analysis was done by one-way ANOVA, post-test Tukey. * $p < 0.05$; ** $p < 0.01$, LTA versus LTA and MMG-11; n.s., not significant. See also Figures S6 and S7 as well as Tables S4 and S5

restore 15-LOX-1 protein levels in these cells indicating that impaired 15-LOX-1 is not due to concomitant elevation of PGE_2 (Figure S10b). *Staphylococcus aureus* treatment did not affect the expression of the CD124, a subunit of the IL-4 receptor (Figure S10c). As mentioned above, phosphorylation of ERK-1/2 that mediated 15-LOX-1 expression in human M2-MDM [36] was moderately influenced by LTA (Figure 6d). Similarly, the phosphorylation of STAT-6, Akt, p70S6 kinase (p70S6K) and cellular myelocytomatosis oncogene (c-Myc) were largely unaffected by LTA (Figure 6d), but of interest, LTA significantly diminished the expression of late endosomal/lysosomal adaptor, MAPK and mTOR activator 1 (Lamtor1) during M2 polarization (Figure 6d).

DISCUSSION

Staphylococcus aureus persistently colonizes ~20% of healthy individuals without provoking any symptoms, while 80% of the population are either transiently colonized or non-carriers [13, 37]. However, *S. aureus* can cause a variety of diseases, ranging from soft tissue infections to severe life-threatening disorders [14]. For instance, *S. aureus* prevalently causes osteomyelitis [20, 21], which frequently develops chronicity despite antimicrobial treatment [22, 23]. To optimize treatment strategies, broader understanding of the complex interactions between *S. aureus* and the host is necessary [16]. Here, we aimed at investigating how *S. aureus* affects LM pathway expression and consequently the respective LM profiles in host cells, and at gaining insights into the molecular mechanisms underlying the modulation of LM networks by *S. aureus*.

We exploited a murine in vivo model of haematogenous osteomyelitis that closely reflects the human disease [24], induced by i.v. infection with the well-characterized *S. aureus* strain 6850. We observed

distinct formation of LM in the acute and the chronic phase, which also depends on the type of tissue. 5-LOX-derived products declined in all examined tissues in the chronic vs. the acute phase, indicating an impaired pro-inflammatory status in the chronic phase. Reduced LTB_4 levels in chronic vs. acute osteomyelitis were evident also in tissue samples of human patients from the osteomyelitic focus [38]. Also, lower amounts of COX-derived products were found in all examined tissues in the chronic vs. acute phase, in contrast to previous studies that reported elevated PGs at the site of bone loss in osteomyelitis models [39].

In bone repair, PG production in the early inflammatory phase was proposed to be involved in bone healing [40]. PGD_2 was the only COX product that increased in the chronic phase, at least in spleen and bone. In fact, PGD_2 has protective, anti-inflammatory effects in the early acute phase of inflammation but exacerbates leukocyte migration, activation and survival in the chronic phase [41–43] implying pro-inflammatory functions for PGD_2 in chronic osteomyelitis. Possibly, the bone cells may try to compensate for the loss of anti-inflammatory and pro-resolving LMs including SPM by elevating the production of PGD_2 . In spleen and lung, several SPM and related 12/15-LOX products were lower in the chronic phase, while a few SPMs (i.e. PD1, PDX, MaR1) were elevated in these organs, to potentially promote resolution of inflammation, bacterial clearance and tissue repair [3, 5, 44]. In contrast, in bone, none of the SPMs were increased in the chronic phase, indicating impaired inflammation resolution, which is in accordance with the X-ray images showing bone destruction. Thus, bone with chronic unresolved infection expressed low levels of SPMs.

To study the modulation of LM pathways by *S. aureus* on the cellular level, we used murine osteoclasts. *Staphylococcus aureus* was shown to infect and proliferate within bone-resorbing osteoclasts by avoiding

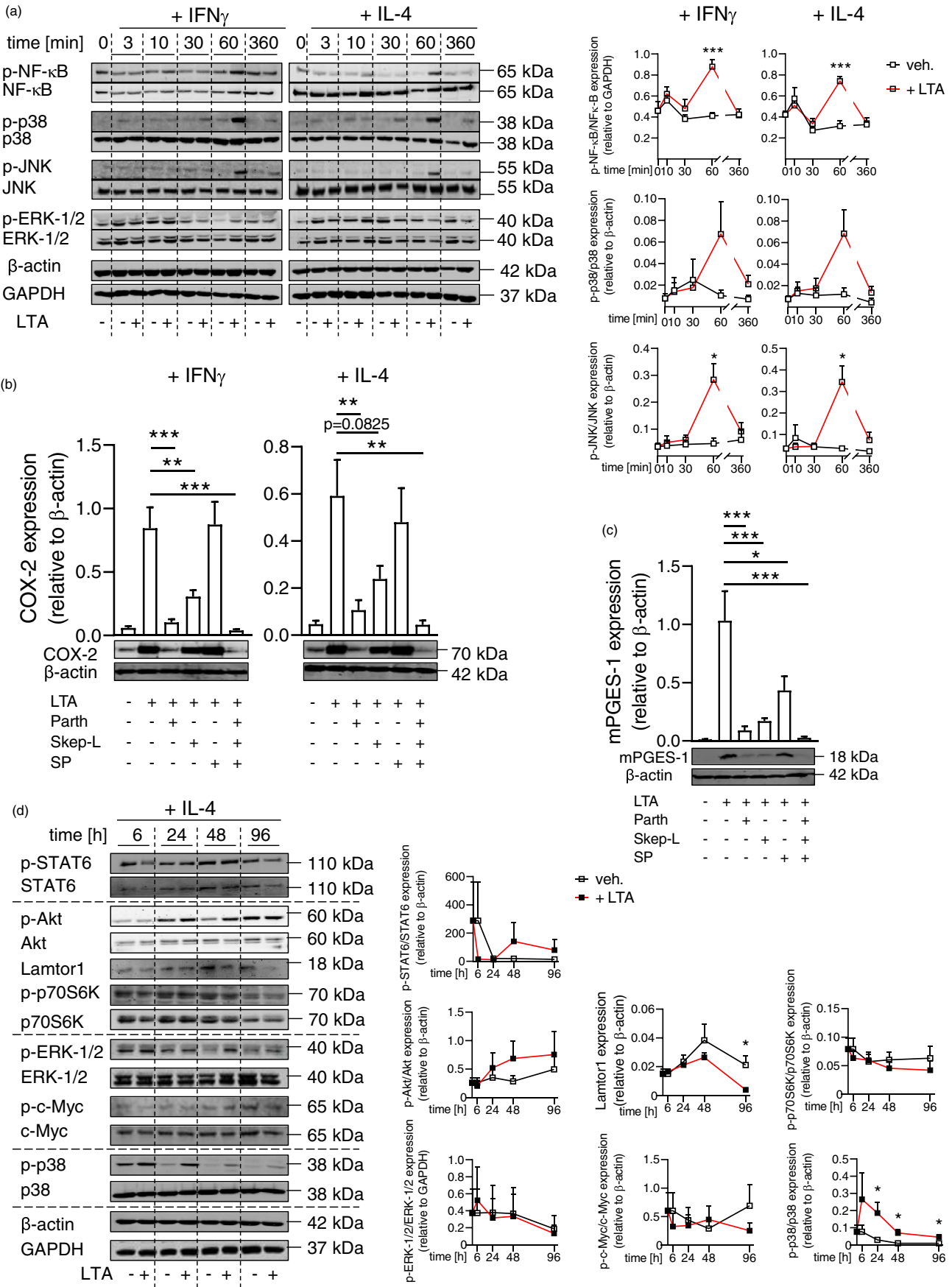


FIGURE 6 *S. aureus*-induced COX-2 and mPGES-1 expression involves NF- κ B and p38 MAPK while downregulation of 15-LOX-1 correlates with Lamtor-1. (a–c) M₀ were treated with IFN- γ or IL-4 in the absence or presence of 1 μ g/ml LTA for the indicated times. (a) Cells were harvested and immunoblotted for phospho-NF- κ B, NF- κ B, phospho-p38 MAPK, p38 MAPK, phospho-JNK, JNK, phospho-ERK-1/2, ERK-1/2, and GAPDH or β -actin. Exemplary results are shown from $n = 3$ –4 separate donors. (b, c) Cells were pre-incubated with 10 μ M parthenolide, 3 μ M SP600125 or 3 μ M skepinone-L for 15 min. After 6 h, cells were immunoblotted for COX-2 (b) and after 48 h, M_{IFN- γ} were immunoblotted for mPGES-1 (c). For densitometric analysis (upper panels, each), COX-2 and mPGES-1 proteins were normalized to β -actin; exemplary results (bottom panels, each) are shown from $n = 5$ separate donors (b), $n = 4$ separate donors (c). One-way ANOVA, post-test Tukey. (d) M₀ were treated with IL-4 in the absence or presence of 1 μ g/ml LTA for the indicated times. Cells were immunoblotted for phospho-STAT-6, STAT-6, phospho-Akt, Akt, Lamtor1, phospho-p70S6K, p70S6K, phospho-ERK-1/2, ERK-1/2, phospho-c-Myc, c-Myc, phospho-p38 MAPK, p38 MAPK, and normalized to β -actin or GAPDH for densitometric analysis. Exemplary results (left panel) and densitometric analysis (right panel) are shown. Data are means + SEM; $n = 3$ –4 separate donors; * $p < 0.05$, LTA versus vehicle. Data were log-transformed for statistical analysis, unpaired Student's t -test. See also Figures S7 and S8

lysosomal compartments, defining a new function of osteoclasts in osteomyelitis as host cells for intracellular bacterial replication [45]. Although osteoclasts are known to respond to LM [46, 47], the generation of LM by osteoclasts in response to bacteria has not been reported so far to the best of our knowledge. We show that untreated osteoclasts produced several types of LM in response to bacterial exotoxins (contained in the SACM [8]), including COX- and 5-LOX-derived LM, while 12/15-LOX products were sparsely formed with no SPM detectable, along with only minute expression of 15-LOX-1. While higher PG formation correlated to enhanced COX-2 and mPGES-1 protein levels, exposure to *S. aureus* decreased 5-LOX-derived LM, although the 5-LOX protein levels remained elevated.

Note that the regio-specificity of murine and human 15-LOX-1 differs, where human 15-LOX-1 oxygenates AA and DHA mainly at carbon C15 and C17, respectively, while the murine orthologue predominantly oxygenates C12 and C14, respectively [35]. Therefore, and due to the very low capacities of the murine osteoclasts to produce LM along with the laborious preparation with low yields of cells, we used human MDM as an alternative cellular model which like osteoclasts derive from the monocyte phagocytic system [17]. In fact, besides osteoclasts also macrophages contribute to *S. aureus*-induced osteomyelitis [27] and *S. aureus* can persist in macrophages [48], supporting evasion of the innate immune system and dissemination of staphylococci [48]. Our data show that exposure to *S. aureus* strikingly increases COX-2 and mPGES-1 protein levels in all MDM phenotypes concomitant with massive PGE₂ formation, but markedly suppresses the levels of 15-LOX-1 protein and its enzymatically formed products. COX-2 and mPGES-1 are strongly co-induced under inflammatory conditions and accomplish the massive formation of PGE₂ at sites of inflammation [49], and both enzymes are strongly expressed in pro-inflammatory M1 macrophages [50, 51]. In contrast, 15-LOX-1 is the key enzyme in SPM formation in macrophages [9] with anti-inflammatory and pro-resolving features [7]. Thus, among LM-biosynthetic

pathways in MDM, *S. aureus* promotes pro-inflammatory enzymes, that is, COX-2 and mPGES-1, but represses pro-resolving ones, that is, 15-LOX-1, which implies an overall inflammatory outcome. This is supported by the concomitant elevation of pro-inflammatory M1 markers CD54 and CD80 and impairment of the anti-inflammatory M2 markers CD163 and CD206 [52], due to exposure of all three MDM phenotypes to *S. aureus*. Elevated COX-2 expression and PGE₂ production due to *S. aureus* infection was found also in nasal tissue fibroblasts [53], murine osteoblasts [54], oral epithelial cells [55] and human aortic endothelial cells [56]. However, the link to elevated mPGES-1 in response to *S. aureus* has not been discovered yet. PGE₂ is a key mediator in chronic infections with pivotal roles for immune cell functions, but like PGD₂, also the actions of PGE₂ are versatile, depending on timing and context: PGE₂ acts pro-inflammatory at early inflammatory stages [57, 58], but may also suppress innate and adaptive immune responses [59, 60]. Notably, PGE₂ inhibited macrophage activation and their ability for phagocytosis and pathogen killing [61], and in oral epithelial cells, PGE₂ promoted growth and adherence of *S. aureus* [55].

The finding that *S. aureus* prevents 15-LOX-1 expression in M_{IL-4} and consequently diminishes SPM formation is novel and implies that such lack of SPM may favour persistence of *S. aureus*, in agreement with persistent infection in sepsis [11, 12]. Indeed, SPMs are highly potent immunoresolvents that promote bacterial killing and phagocytosis, for example in skin infections, where SPMs enhanced vancomycin-mediated clearance of *S. aureus* [1]. In addition, the impaired generation of LTB₄ due to *S. aureus* may favour bacterial survival, since macrophage-derived LTB₄ promoted clearance of *S. aureus* in a mouse model of skin infection [62].

Our results with heat-attenuated *S. aureus* show that the modulatory effects on MDM are seemingly caused by bacterial component(s) without requiring vital bacteria. We found that LTA mimicked *S. aureus*-induced alteration of LM-biosynthetic pathways and cytokine release in MDM. Note that exogenous LTA at 1 μ g/ml was



more efficient to induce MDM cytotoxicity and IL-10 release than infection with *S. aureus*, possibly due to somewhat lower LTA release (approximately 0.3–0.5 $\mu\text{g/ml}$) at MOI of 2 in the latter case. LTA binds to TLR-2 and is required for normal cell morphology, growth and division of *S. aureus* [19, 29] and is released by *S. aureus* and various Gram-positive bacteria during growth [63, 64]. LTA induces inflammatory responses and causes secretion of inflammatory cytokines such as TNF α , IL-6, IL-1 β and IL-10 from various leukocytes [29, 65–67]. Our data confirm substantial release of TNF α , IL-6, IL-1 β and IL-10 by LTA and reveal a role in regulating inflammation by modulation of LM-biosynthetic pathways in different macrophage phenotypes. IL-10 is generally considered as an anti-inflammatory cytokine but can also contribute to *S. aureus* persistence [68] and high IL-10 production was associated with sustained chronic infections where its blockade promoted pathogen clearance [69]. LTA strikingly elevated COX-2 and mPGES-1 protein levels along with massive induction of PGE₂ formation. While induction of COX-2 expression by LTA was also reported for human gingival fibroblasts [70], murine RAW264.7 macrophages [71], and BV-2 microglia [72], elevation of mPGES-1 protein levels and blocking of 15-LOX-1 expression by LTA has not been reported before in any cell type.

We provide evidence that the rapid and pronounced upregulation of COX-2 and mPGES-1 by LTA in MDM involves NF- κ B and p38 MAPK signalling pathways. First, in agreement with the literature [29, 30, 71, 73–77], we show that LTA, particularly after 1 h of incubation, causes robust but transient activation of NF- κ B, JNK and p38 MAPK, but not of ERK-1/2. These findings are in line with those of earlier reports, documenting *S. aureus* to induce phosphorylation of NF- κ B, JNK and p38 MAPK [56, 78]. Second, inhibition of the NF- κ B and p38 MAPK pathways in MDM strongly prevented LTA-induced COX-2 and mPGES-1 induction; JNK inhibition was without effect (COX-2) or less efficient (mPGES-1). Due to the almost complete block of COX-2 and mPGES-1 expression by inhibiting NF- κ B, we assume that rather sequential than synergistic action of NF- κ B and p38 MAPK is operative, supported by the finding that p38 MAPK acts upstream of NF- κ B in primary neonatal rat cardiac myocytes [79]. Investigation of pathways regulating the expression of 15-LOX-1 revealed that LTA diminishes the expression of Lamtor1 during M2 polarization. Interestingly, Lamtor1 was shown to be required for M2 polarization in murine bone marrow-derived macrophages [80]. Although we are unable to clearly define the pathways linking LTA signalling to reduced 15-LOX-1 expression, our results suggest that Lamtor1 may be connected to the modulation of 15-LOX-1 expression by *S. aureus*, which requires more detailed studies and remains to be investigated in the future.

Taken together, we show that *S. aureus*-induced murine osteomyelitis in vivo is associated with massive generation of broad range of LM with distinct LM signature profiles in acute and chronic phases. Experiments on the cellular level with monocyte-derived cells reveal that *S. aureus* modulates the expression of LM pathways towards a pro-inflammatory pattern, seemingly mediated by LTA. In particular, pro-inflammatory COX-2 and mPGES-1 pathways are upregulated with massive PGE₂ formation among a broad spectrum of LM, while IL-4-induced 15-LOX-1 expression is impaired along with lower formation of SPM. These results help to explain how *S. aureus* infections mediate the inflammatory reactions associated with infectious diseases and will be of relevance for pharmacological interventions with *S. aureus* infections by adjusting favourable LM profiles besides or in combination with antibiotics.

MATERIALS AND METHODS

Bacterial strains

The methicillin-susceptible *S. aureus* strain 6850, a wild-type isolate from a patient with osteomyelitis, was originally produced by R. Proctor [81]. For experiments with intact *S. aureus*, bacteria were grown for 14 h at 37°C in brain heart infusion broth (BHI) (Sigma-Aldrich) while shaking. The culture was diluted to an OD_{600nm} of 0.05 and grown for another 3 h (log-phase). Bacteria were washed with PBS and resuspended in PBS. To prepare *S. aureus*-conditioned medium (SACM), bacteria were grown for 24 h in medium, diluted to an OD_{600nm} of 0.05 and grown for another 24 h, pelleted for 5 min at 3350 \times g, and sterile-filtered through a Millex-GP filter unit (0.22 μm ; Millipore) prior to use.

Murine cells

For isolation of murine osteoclast, femur and tibia were cleaned by removing the tissue and disinfecting them with 70% ethanol. The epiphysis was removed. Bones of one animal were transferred to a 0.5 ml Eppendorf tube, which was prepared by pushing a 18G-needle through the bottom and placing it in a 1.5 ml Eppendorf tube. The bone marrow was removed by centrifugation (10 000 \times g, 15 min). The supernatant was discarded, and bone marrow cells (BMC) were resuspended in an adequate amount of medium. Cells were counted and seeded at a density of 2×10^6 cells in a 10 cm-Petri dish in proliferation medium (DMEM; Sigma-Aldrich), 10% foetal calf serum (FCS) (v/v), 100 U/ml penicillin and 100 $\mu\text{g/ml}$ streptomycin (Biochrom/Merck). The day following the isolation, cells

from the supernatant of a 10 cm dish were centrifuged (1000 × g, 5 min), resuspended and seeded in differentiation medium (DMEM), 10% FCS (v/v), 100 U/ml penicillin, 100 µg/ml streptomycin, 50 ng/ml M-CSF and 20 ng/ml RANKL (PeproTech, Hamburg, Germany) at a density of 2×10^6 cells/well on 6-well plates. The medium was carefully replaced after 3 days by removing only 70–80% of the medium and filling up with fresh differentiation medium. The infection with *S. aureus* was started at day 7 after seeding in differentiation medium.

Human cells

Monocytes were isolated from leukocyte concentrates derived from freshly withdrawn peripheral blood of healthy adult male and female donors (Institute of Transfusion Medicine, Jena University Hospital, Germany) as reported before [82]. The experimental protocol for isolation of human blood cells was approved by the ethical committee of the Jena University Hospital (5050-01/17; March 3, 2017). All methods were performed in accordance with the relevant guidelines and regulations. In brief, peripheral blood mononuclear cells (PBMCs) were separated using dextran sedimentation, followed by centrifugation on lymphocyte separation medium (Histopaque[®]-1077, Sigma-Aldrich). PBMCs were seeded in PBS supplemented with 1 mM Ca²⁺ and 0.5 mM Mg²⁺ in cell culture flasks (Greiner Bio-one, Frickenhausen, Germany) for 1.5 h at 37°C and 5% CO₂ for adherence of monocytes. For differentiation of monocytes to MDM and polarization towards M1- and M2-like cells, published criteria were used [9, 52]. M0 were generated by incubating monocytes with 10 ng/ml GM-CSF (PeproTech, Hamburg, Germany) and 10 ng/ml M-CSF (PeproTech, Hamburg, Germany) for 5 days in RPMI 1640 (Sigma-Aldrich) supplemented with 5% (v/v) heat-inactivated FCS, 100 U/ml penicillin and 100 µg/ml streptomycin (Biochrom/Merck). When starting the infection with *S. aureus*, MDMs were grown without cytokines (M₀), polarized with 20 ng/ml IFN-γ (PeproTech, Hamburg, Germany) to obtain M1-like MDM (M_{IFN-γ}) or with 20 ng/ml IL-4 (PeproTech) to obtain M2-like MDM (M_{IL-4}).

Incubation of human monocyte-derived macrophages and murine osteoclasts

Following differentiation, human MDMs were seeded ($2 \times 10^6/2$ ml) in X-VIVO 15 containing L-glutamine without gentamicin or phenolred (Biozym/LONZA, #BE02-061Q) supplemented with 5% (v/v) FCS in 6-well plates (Greiner Bio-one). *Staphylococcus aureus* (for MDM MOI 2; for osteoclasts MOI 10), attenuated *S. aureus* (heat

inactivated for 10 min at 95°C, MOI 2) or 1 µg/ml LTA from *S. aureus* (L2515, Sigma-Aldrich) were added at 37°C. Simultaneously, polarization agents were added to MDM as described above. After infection with *S. aureus* for 2 h, cells were treated with 20 µg/ml recombinant lysostaphin (WAK-Chemie Medical GmbH, Steinbach, Taunus, Germany) in PBS for 30 min at 37°C to remove extracellular bacteria. Cells were further cultivated without (M₀, osteoclasts) or with polarization agents (M_{IFN-γ}, M_{IL-4}) for the indicated times (for MDM in X-VIVO supplemented with 5% (v/v) FCS, 100 U/ml penicillin and 100 µg/ml streptomycin; for osteoclasts in DMEM supplemented with 10% FCS (v/v), 100 U/ml penicillin and 100 µg/ml streptomycin). For measurement of LM, 1 ml of the cell culture medium was collected. In addition, to evoke LM biosynthesis, remaining culture medium was removed, cells were washed with PBS and treated with SACM (1%, 90 min for MDM; 0.5%, 60 min for osteoclasts) in 1 ml PBS plus 1 mM CaCl₂ at 37°C.

LM metabolomics

Supernatants (1 ml) of the incubations were immediately transferred to 2 ml of ice-cold methanol containing the deuterium-labelled internal standards (200 nM d8-5S-HETE, d4-LTB₄, d5-LXA₄, d5-RvD2, d4-PGE₂ and 10 µM d8-AA). Sample preparation was carried out by adapting published criteria [9]. In brief, samples were kept at –20°C for 60 min to allow protein precipitation. After centrifugation (1200×g, 10 min, 4°C), 9 ml acidified H₂O was added (final pH 3.5) and samples were subjected to solid phase extraction. Solid phase cartridges (Sep-Pak[®] Vac 6cc 500 mg/6 ml C18; Waters, Milford, MA) were equilibrated with 6 ml methanol and 2 ml H₂O before samples were loaded onto columns. After washing with 6 ml H₂O and additional 6 ml *n*-hexane, LMs were eluted with 6 ml methyl formate. Finally, the samples were brought to dryness using an evaporation system (TurboVap LV, Biotage, Uppsala, Sweden) and resuspended in 100 µl methanol-water (50/50, v/v) for UPLC-MS/MS automated injections. LM profiling was analysed with an Acquity[™] UPLC system (Waters, Milford, MA, USA) and a QTRAP 5500 Mass Spectrometer (ABSciex, Darmstadt, Germany) equipped with a Turbo V[®] Source and electrospray ionization. LMs were eluted using an ACQUITY UPLC[®] BEH C18 column (1.7 µm, 2.1 × 100 mm; Waters, Eschborn, Germany) at 50°C with a flow rate of 0.3 ml/min and a mobile phase consisting of methanol–water–acetic acid of 42:58:0.01 (v/v/v) that was ramped to 86:14:0.01 (v/v/v) over 12.5 min and then to 98:2:0.01 (v/v/v) for 3 min [51]. The QTrap 5500 was operated in negative ionization mode using scheduled multiple reaction monitoring (MRM) coupled

with information-dependent acquisition. The scheduled MRM window was 60 s, optimized LM parameters were adopted [51] and the curtain gas pressure was set to 35 psi. The retention time and at least six diagnostic ions for each LM were confirmed by means of an external standard (Cayman Chemical/Biomol GmbH, Hamburg, Germany). Quantification was achieved by calibration curves for each LM. Linear calibration curves were obtained for each LM and gave r^2 values of 0.998 or higher (for fatty acids 0.95 or higher), and the limit of detection for each targeted LM was determined, as previously reported by us [51].

SDS-PAGE and Western blot

Cell lysates of MDM corresponding to 2×10^6 cells were separated on 16% polyacrylamide gels (5-LOX, FLAP, COX-1, 15-LOX-1, mPGES-1, phospho-Akt, Akt, Lamtor1), 10% polyacrylamide gels (15-LOX-2, LTA₄H, phospho-NF- κ B, NF- κ B, phospho-JNK, JNK, phospho-p38 MAPK, p38 MAPK, phospho-ERK-1/2, ERK-1/2, phospho-c-Myc, c-Myc, phospho-p70S6K, p70S6K) and 8% polyacrylamide gels (cPLA₂ α , COX-2, phospho-STAT-6, STAT-6). Cell lysates of murine osteoclasts corresponding to 2×10^6 cells were separated on 16% polyacrylamide gels (COX-1, mPGES-1) and 10% polyacrylamide gels (COX-2, 15-LOX, 5-LOX). Gels were blotted onto nitrocellulose membranes (Amersham™ Protran Supported 0.45 μ m nitrocellulose, GE Healthcare, Freiburg, Germany). The membranes were incubated with the following primary antibodies for human MDM samples: rabbit polyclonal anti-5-LOX, 1:1000 (by Genscript, Piscataway to a peptide with the C-terminal 12 amino acids of 5-LOX: CSPDRIPNSVAI); rabbit polyclonal anti-FLAP, 1:1000 (ab85227, Abcam, Cambridge, UK); rabbit polyclonal anti-COX-1, 1:1000 (#4841, Cell Signaling, Danvers, MA); mouse monoclonal anti-15-LOX-1, 1:200 (ab119774, Abcam); rabbit polyclonal anti-mPGES-1, 1:5000 (kindly provided by Prof. Per-Johan Jakobsson, Karolinska Institutet, Stockholm, Sweden); rabbit polyclonal anti-phospho-Akt (Ser473), 1:750 (#9271, Cell Signaling); mouse monoclonal anti-Akt, 1:1000 (40D4, #2920, Cell Signaling); rabbit monoclonal anti-Lamtor1/C11orf59, 1:1000 (D11H6, #8975, Cell Signaling); rabbit polyclonal anti-15-LOX-2, 1:200 (ab23691, Abcam); rabbit monoclonal anti-LTA₄H, 1:1000 (ab133512, Abcam); mouse monoclonal anti-phospho-NF- κ B p65 (Ser536), 1:750 (7F1, #3036, Cell Signaling); rabbit monoclonal anti-NF- κ B p65, 1:1000 (C22B4, #4764, Cell Signaling); rabbit polyclonal anti-phospho-SAPK/JNK (Thr183/Tyr185), 1:750 (#9251, Cell Signaling); rabbit polyclonal anti-SAPK/JNK, 1:1000 (#9252, Cell Signaling); rabbit polyclonal anti-phospho-p38 MAPK (Thr180/Tyr182), 1:750 (#9211, Cell Signaling); rabbit monoclonal anti-p38 MAPK, 1:1000

(D13E1, #8690, Cell Signaling); mouse monoclonal anti-phospho-p44/42 MAPK (ERK-1/2) (Thr202/Tyr204), 1:750 (#9106, Cell Signaling); rabbit monoclonal anti-p44/42 MAPK (ERK-1/2), 1:1000 (#4695, Cell Signaling); rabbit polyclonal anti-phospho-c-Myc (Thr85), 1:1000 (#PA5-36673, Thermo Fisher Scientific, Waltham, MA); rabbit monoclonal anti-c-Myc, 1:1000 (D84C12, #5605, Cell Signaling); mouse monoclonal anti-phospho-p70s6k (Thr389), 1:200 (1A5, #9206, Cell Signaling); rabbit monoclonal anti-p70s6k, 1:1000 (49D7, #2708, Cell Signaling); rabbit polyclonal anti-cPLA₂ α , 1:200 (#2832, Cell Signaling); rabbit monoclonal anti-COX-2, 1:500 (D5H5, #12282, Cell Signaling); rabbit polyclonal anti-phospho-STAT6 (Tyr641), 1:1000 (#9361, Cell Signaling); mouse polyclonal anti-STAT6, 1:200 (ab88540, Abcam); mouse monoclonal anti- β -actin, 1:1000 (8H10D10, #3700, Cell Signaling); and rabbit monoclonal anti-GAPDH, 1:1000 (D16H11, #5174, Cell Signaling). The membranes were incubated with the following primary antibodies for murine osteoclast samples: rabbit polyclonal anti-COX-1, 1:1000 (#4841, Cell Signaling); rabbit polyclonal anti-COX-2, 1:1000 (#4842, Cell Signaling); rabbit monoclonal anti-mPGES-1, 1:1000 (ab180589, Abcam); rabbit polyclonal anti-15-LOX-1, 1:200 (ab80221, Abcam); mouse monoclonal anti-5-LOX, 1:1000 (#610694, BD Biosciences); and mouse monoclonal anti- β -actin, 1:1000 (8H10D10, #3700, Cell Signaling). Immunoreactive bands were stained with following secondary antibodies: IRDye 800CW Goat anti-Rabbit IgG (H + L), 1:15 000 (926–32211, LI-COR Biosciences, Lincoln, NE); IRDye 800CW Goat anti-Mouse IgG (H + L), 1:15 000 (926–32210, LI-COR Biosciences); and/or IRDye 680LT Goat anti-Mouse IgG (H + L), 1:40 000 (926–68020, LI-COR Biosciences), and visualized by an Odyssey infrared imager (LI-COR Biosciences). Data from densitometric analysis were background corrected.

Analysis of LTA by Western blot

To determine the amount of LTA in SACM and intact *S. aureus*, a well-established method was used [83]. *Staphylococcus aureus* was grown in BHI for 24 h. Then, the culture was diluted to an OD_{600nm} of 0.05 and grown for another 4 h or 24 h. To analyse LTA from the supernatants, 5 ml of the bacteria culture was centrifuged (3016 g, 5 min) to pellet the bacteria. 10 μ l supernatant was mixed with 1.25 μ l PBS and 3.75 μ l 4 \times Laemmli sample buffer (2% SDS sample buffer). To analyse LTA from intact bacteria, 1 ml of culture aliquots was lysed with 0.5 ml of 0.1 mm silica glass beads (BeadBug™ pre-filled tubes, 2.0 ml capacity, Sigma-Aldrich) by vortex mixing (45 min, 1°C). Samples were centrifuged (200 \times g, 1 min) to sediment glass beads. 0.5 ml of supernatant was transferred to a new reaction

tube (Eppendorf, Hamburg, Germany) and centrifuged ($16\,000 \times g$, 10 min) to collect bacterial debris containing cell-associated LTA. The pellet was suspended in 1x Laemmli sample buffer. Samples were normalized for OD values (more precisely: a sample from a culture with an OD of 1 was suspended in $15\ \mu\text{l}$ 1x Laemmli sample buffer). Samples were boiled (30 min, 95°C) and centrifuged ($16\,000 \times g$, 5 min) to remove insoluble material. $15\ \mu\text{l}$ samples from supernatants and $10\ \mu\text{l}$ samples from intact *S. aureus* were separated on 16% polyacrylamide gels. Different amounts of LTA from *S. aureus* (L2515, Sigma-Aldrich), in the range of 10–1000 ng, were loaded to allow quantification of LTA in supernatants and intact *S. aureus*. For LTA detection, the membranes were incubated with mouse monoclonal anti-Gram-positive bacteria LTA antibody, 1:50 (clone G43J, #MA1-7402, Thermo Fisher). Immunoreactive bands were stained and visualized as described above.

Analysis of cell viability

To analyse cell viability, MDMs ($2 \times 10^6/2\ \text{ml}$; $100\ \mu\text{l}$ per well) were incubated with the test compounds in 96-well plates. At the indicated time points, the cells were incubated with 3-(4,5-dimethylthiazol-2-yl)-2,5-diphenyltetrazolium bromide (MTT, 5 mg/ml in PBS, $20\ \mu\text{l}$ per well) for 3 h. Then, SDS lysis buffer (10% SDS in 20 mM HCl; pH 4.5; $100\ \mu\text{l}$ per well) was added for 20 h at 175 rpm. Absorption was measured at 570 nm using Multiskan Spectrum (Thermo Fisher). Cell culture medium was used as negative control. Cell viability was calculated by setting the untreated control to 100%.

Counting of intracellular bacteria

The MDMs were detached by treatment with PBS plus 5 mM EDTA (20 min, 37°C), counted and lysed with water. Cell lysates were plated on Columbia blood agar plates in certain dilutions (0 h: 10^{-3} , 10^{-4} ; 6 h: 10^{-4} ; 24 h: 10^{-3} , 10^{-2} ; 48 h: 10^{-2} ; 96 h: 10^{-1}) to determine bacterial loads. Bacterial colonies were counted using Colony Quant (Schuett-Biotec, Göttingen, Germany).

Flow cytometry analysis

The MDMs were detached by treatment with PBS plus 0.5% BSA, 5 mM EDTA and 0.1% sodium azide (20 min, 37°C). To determine the viability, the cells were resuspended in $20\ \mu\text{l}$ Zombie Aqua Fixable Viability Kit (#423102, BioLegend, San Diego, CA) for 5 min. Non-specific antibody binding was blocked with mouse serum (5 min, 4°C)

prior to antibody staining. Then, MDMs were stained with fluorochrome-labelled antibody mixtures (20 min, 4°C). The following antibodies were used: FITC mouse monoclonal anti-human CD14 ($20\ \mu\text{l}/\text{test}$, clone M5E2, #555397, BD Biosciences, San Jose, CA); APC-H7 mouse monoclonal anti-human CD80 (5 $\mu\text{l}/\text{test}$, clone L307.4, #561134, BD Biosciences); PE/Cy7 mouse monoclonal anti-human CD54 (5 $\mu\text{l}/\text{test}$, clone HA58, #353116, BioLegend); APC mouse monoclonal anti-human CD206 (20 $\mu\text{l}/\text{test}$, clone 19.2, #550889, BD Biosciences); PE mouse monoclonal anti-human CD163 (20 $\mu\text{l}/\text{test}$, clone GHI/61, #556018, BD Biosciences); APC mouse monoclonal anti-human CD124 (10 $\mu\text{l}/\text{test}$, clone G077F6, #355005, BioLegend); and FITC mouse monoclonal anti-human CD282 (5 $\mu\text{l}/\text{test}$, clone TL2.1, #309705, BioLegend). Fluorescent staining for flow cytometric analysis of MDM was performed in FACS buffer (PBS plus 0.5% BSA, 5 mM EDTA and 0.1% sodium azide). After staining, cells were fixed with 4% paraformaldehyde (10 min, 4°C). MDMs were analysed using BD LSR Fortessa (BD Biosciences), and data were analysed using FlowJo X Software (BD Biosciences).

Cytokine release

For measurement of the cytokine levels, supernatants were collected and centrifuged ($21\,130\ g$, 4°C , 5 min). The levels of released TNF α , IL-6, IL-1 β and IL-10 were analysed by in-house-made ELISA kits (R&D Systems, Bio-Techne). The amounts of cytokines were calculated using standard curves.

Animals

Female C57BL/6 mice at the age of 10–12 weeks ($n = 3\text{--}5$ per experimental group) were housed in a controlled environment ($21 \pm 2^\circ\text{C}$) and provided with standard rodent chow and water. Animals were allowed to acclimate for 4 days prior to experiments and were subjected to 12-h light/12-h dark schedule. Mice were randomly assigned for the experiments, which were conducted during the light phase. The experimental procedures for mouse studies were approved by German regulations of the Society for Laboratory Animal Science 22-2684-04-02-006/15 and 22-2684-04-02-046/16 (Thuringia, Jena).

Acute and chronic osteomyelitis in mice and tissue sample preparation

Mice received *S. aureus* (strain 6850, $10^6\ \text{CFU}/200\ \mu\text{l}$) by i.v. injection according to well-recognized experimental

design for studying acute and chronic osteomyelitis [24]. After 1 week (acute phase) and 6 weeks (chronic phase), mice were sacrificed by inhalation of CO₂. Spleen, lung and bone were isolated, cut into small pieces, and approximately 40 mg of each sample was weighted. 20 µl methanol was added per 1 mg sample in plastic tubes, and samples were homogenized using ULTRA-TURRAX[®] tissue homogenizer (Sigma-Aldrich, Taufkirchen, Germany). Homogenized tissues were filled up to 1 ml with PBS. 10 µl of deuterium-labelled LM standards (200 nM d8-5S-HETE, d4-LTB₄, d5-LXA₄, d5-RvD2, d4-PGE₂ and 10 µM d8-AA) was added as internal reference. Samples were stored at -20°C overnight to allow protein precipitation prior to SPE and LM assessment using UPLC-MS/MS analysis as described above.

Statistics

Results are expressed as mean ± standard error of the mean (SEM) of n observations, where n represents the number of experiments with separate donors, performed on different days, as indicated. Analyses of data were conducted using GraphPad Prism 8 software (San Diego, CA). Grubbs outlier test (alpha = 0.05) was used to identify outliers. Normality of data distribution was tested with Shapiro-Wilk test. Two-tailed paired or unpaired Student's t-test test or Mann-Whitney U Test was applied for comparison of two groups. For multiple comparison, one-way analysis of variance (ANOVA) with Tukey's post-hoc tests were applied as indicated. The criterion for statistical significance is $p < 0.05$.

ACKNOWLEDGEMENTS

We thank S. Wendler and P. Wiecha for excellent technical assistance. Open access funding enabled and organized by Projekt DEAL.

CONFLICT OF INTEREST

The authors declare no competing financial interest.

AUTHOR CONTRIBUTIONS

J.G., O.W., C.N.S., L.T. and B.L. designed the study. L.M. and K.G. performed the analysis of LM profiles. L.M. and T.B. performed the Western Blot analysis. P.M.J performed the FACS experiments and evaluated the FACS data. L.M. performed the ELISA analysis. T.B. and D.K. performed the MTT assays. J.G. and L.M. performed the data analysis, statistics and prepared graphs. L.T. supplied the bacterial strain and murine osteoclasts. S.P. and V.H. designed and performed the animal experiments. L.M. and O.W. wrote the manuscript and C.N.S. and L.T.

edited the manuscript, all authors contributed to manuscript preparation.

ETHICAL APPROVAL

The experimental protocol for isolation of human blood cells was approved by the ethical committee of the Jena University Hospital (5050-01/17; 3 March 2017). The experimental procedures for mouse studies were approved by German regulations of the Society for Laboratory Animal Science 22-2684-04-02-006/15 and 22-2684-04-02-046/16 (Thuringia, Jena).

ORCID

Paul M. Jordan  <https://orcid.org/0000-0002-8364-4236>

Kerstin Günther  <https://orcid.org/0000-0001-8230-5972>

Oliver Werz  <https://orcid.org/0000-0002-5064-4379>

REFERENCES

- Chiang N, Fredman G, Bäckhed F, Oh SF, Vickery T, Schmidt BA, et al. Infection regulates pro-resolving mediators that lower antibiotic requirements. *Nature*. 2012;484:524–8.
- Medzhitov R. Origin and physiological roles of inflammation. *Nature*. 2008;454:428–35.
- Serhan CN. Pro-resolving lipid mediators are leads for resolution physiology. *Nature*. 2014;510:92–101.
- Funk CD. Prostaglandins and leukotrienes: advances in eicosanoid biology. *Science*. 2011;294:1871–5.
- Serhan CN, Levy BD. Resolvins in inflammation: emergence of the pro-resolving superfamily of mediators. *J Clin Invest*. 2018;128:2657–69.
- Serhan CN, Chiang N, Dalli J. The resolution code of acute inflammation: Novel pro-resolving lipid mediators in resolution. *Sem Immunol*. 2015;27:200–15.
- Ackermann JA, Hofheinz K, Zaiss MM, Kronke G. The double-edged role of 12/15-lipoxygenase during inflammation and immunity. *Biochim Biophys Acta Mol Cell Biol Lipids*. 2017;1862:371–81.
- Jordan PM, Gerstmeier J, Pace S, Bilancia R, Rao Z, Börner F, et al. Staphylococcus aureus-derived α-hemolysin evokes generation of specialized pro-resolving mediators promoting inflammation resolution. *Cell Rep*. 2020;33(2):108247.
- Werz O, Gerstmeier J, Liberos S, De la Rosa X, Werner M, Norris PC, et al. Human macrophages differentially produce specific resolvins or leukotriene signals that depend on bacterial pathogenicity. *Nat Commun*. 2018;9:59.
- Lee CR, Zeldin DC. Resolving infectious inflammation by targeting the host response. *N Engl J Med*. 2015;373:2183–5.
- Dalli J, Chiang N, Serhan CN. Elucidation of novel 13-series resolvins that increase with atorvastatin and clear infections. *Nat Med*. 2015;21:1071–5.
- Spite M, Norling LV, Summers L, Yang R, Cooper D, Petasis NA, et al. Resolvin D2 is a potent regulator of leukocytes and controls microbial sepsis. *Nature*. 2009;461:1287–91.
- Knox J, Uhlemann AC, Lowy FD. Staphylococcus aureus infections: transmission within households and the community. *Trends Microbiol*. 2015;23:437–44.

14. Tong SYC, Davis JS, Eichenberger E, Holland TL, Fowler VG Jr. Staphylococcus aureus infections: epidemiology, pathophysiology, clinical manifestations, and management. *Clin Microbiol Rev.* 2015;28:603–61.
15. DeLeo FR, Chambers HF. Reemergence of antibiotic-resistant Staphylococcus aureus in the genomics era. *J Clin Invest.* 2009;119:2464–74.
16. Miller LS, Fowler VG, Shukla SK, Rose WE, Proctor RA. Development of a vaccine against Staphylococcus aureus invasive infections: Evidence based on human immunity, genetics and bacterial evasion mechanisms. *FEMS Microbiol Rev.* 2020;44:123–53.
17. Boyle WJ, Simonet WS, Lacey DL. Osteoclast differentiation and activation. *Nature.* 2003;423:337–42.
18. Ginsburg I. Role of lipoteichoic acid in infection and inflammation. *Lancet Infect Dis.* 2002;2:171–9.
19. Percy MG, Grundling A. Lipoteichoic acid synthesis and function in gram-positive bacteria. *Annu Rev Microbiol.* 2014;68:81–100.
20. Josse J, Velard F, Gangloff SC. Staphylococcus aureus vs. Osteoblast: Relationship and Consequences in Osteomyelitis. *Front Cell Infect Microbiol.* 2015;5:85.
21. Lew DP, Waldvogel FA. Osteomyelitis. *Lancet.* 2004;364:369–79.
22. Ellington JK, Harris M, Hudson MC, Vishin S, Webb LX, Sherertz R. Intracellular Staphylococcus aureus and antibiotic resistance: implications for treatment of staphylococcal osteomyelitis. *J Orthop Res.* 2006;24:87–93.
23. Sheehy SH, Atkins BA, Bejon P, Byren I, Wyllie D, Athanasou NA, et al. The microbiology of chronic osteomyelitis: prevalence of resistance to common empirical anti-microbial regimens. *J Infect.* 2010;60:338–43.
24. Horst SA, Hoerr V, Beineke A, Kreis C, Tuchscher L, Kalinka J, et al. A novel mouse model of Staphylococcus aureus chronic osteomyelitis that closely mimics the human infection: an integrated view of disease pathogenesis. *Am J Pathol.* 2012;181:1206–14.
25. Kim J, Chaurasia AK, Batool N, Ko KS, Kim KK. Alternative enzyme protection assay to overcome the drawbacks of the gentamicin protection assay for measuring entry and intracellular survival of Staphylococci. *Infect Immun.* 2019;87:e00119–19.
26. Schaffner W, Melly MA, Hash JH, Koenig MG. Lysostaphin: an enzymatic approach to staphylococcal disease. I. In vitro studies. *Yale J Biol Med.* 1967;39:215–29.
27. Wiggers EC, Johnson W, Tucci M, Benghuzzi H. Biochemical and morphological changes associated with macrophages and osteoclasts when challenged with infection. *Biomed Sci Instrum.* 2011;47:183–8.
28. Kubatzky KF, Uhle F, Eigenbrod T. From macrophage to osteoclast - How metabolism determines function and activity. *Cytokine.* 2018;112:102–15.
29. Schwandner R, Dziarski R, Wesche H, Rothe M, Kirschning CJ. Peptidoglycan- and lipoteichoic acid-induced cell activation is mediated by toll-like receptor 2. *J Biol Chem.* 1999;274:17406–9.
30. Wang JE, Dahle MK, McDonald M, Foster SJ, Aasen AO, Thiemermann C. Peptidoglycan and lipoteichoic acid in gram-positive bacterial sepsis: receptors, signal transduction, biological effects, and synergism. *Shock.* 2003;20:402–14.
31. Cheng HF, Wang JL, Zhang MZ, McKanna JA, Harris RC. Role of p38 in the regulation of renal cortical cyclooxygenase-2 expression by extracellular chloride. *J Clin Invest.* 2000;106:681–8.
32. Hunot S, Vila M, Teismann P, Davis RJ, Hirsch EC, Przedborski S, et al. JNK-mediated induction of cyclooxygenase 2 is required for neurodegeneration in a mouse model of Parkinson's disease. *Proc Natl Acad Sci USA.* 2004;101:665–70.
33. Jung YJ, Isaacs JS, Lee S, Trepel J, Neckers L. IL-1 β -mediated up-regulation of HIF-1 α via an NF- κ B/COX-2 pathway identifies HIF-1 as a critical link between inflammation and oncogenesis. *FASEB J.* 2003;17:2115–7.
34. Yang T, Huang Y, Heasley LE, Berl T, Schnermann JB, Briggs JP. MAPK mediation of hypertonicity-stimulated cyclooxygenase-2 expression in renal medullary collecting duct cells. *J Biol Chem.* 2000;275:23281–6.
35. Ivanov I, Kuhn H, Heydeck D. Structural and functional biology of arachidonic acid 15-lipoxygenase-1 (ALOX15). *Gene.* 2015;573:1–32.
36. Rao Z, Pace S, Jordan PM, Bilancia R, Troisi F, Börner F, et al. Vacuolar (H⁺)-ATPase Critically Regulates Specialized Proresolving Mediator Pathways in Human M2-like Monocyte-Derived Macrophages and Has a Crucial Role in Resolution of Inflammation. *J Immunol.* 2019;203:1031–43.
37. Otto M. Staphylococcus colonization of the skin and antimicrobial peptides. *Expert Rev Dermatol.* 2010;5:183–95.
38. Klosterhalfen B, Peters KM, Tons C, Hauptmann S, Klein CL, Kirkpatrick CJ. Local and systemic inflammatory mediator release in patients with acute and chronic posttraumatic osteomyelitis. *J Trauma.* 1996;40:372–8.
39. Norrdin RW, Jee WS, High WB. The role of prostaglandins in bone in vivo. *Prostaglandins, Leukot Essential Fatty Acids.* 1990;41:139–49.
40. Xie C, Ming X, Wang Q, Schwarz EM, Guldberg RE, O'Keefe RJ, et al. COX-2 from the injury milieu is critical for the initiation of periosteal progenitor cell mediated bone healing. *Bone.* 2008;43:1075–83.
41. Ajuebor MN, Singh A, Wallace JL. Cyclooxygenase-2-derived prostaglandin D(2) is an early anti-inflammatory signal in experimental colitis. *Am J Physiol Gastrointest Liver Physiol.* 2000;279:G238–44.
42. Murata T, Aritake K, Tsubosaka Y, Maruyama T, Nakagawa T, Hori M, et al. Anti-inflammatory role of PGD2 in acute lung inflammation and therapeutic application of its signal enhancement. *Proc Natl Acad Sci USA.* 2013;110:5205–10.
43. Sarashina H, Tsubosaka Y, Omori K, Aritake K, Nakagawa T, Hori M, et al. Opposing immunomodulatory roles of prostaglandin D2 during the progression of skin inflammation. *J Immunol.* 2014;192:459–65.
44. Dalli J, Serhan CN. Macrophage proresolving mediators—the when and where. *Microbiol Spectr.* 2016;4.
45. Krauss JL, Roper PM, Ballard A, Shih CC, Fitzpatrick JAJ, Cassat JE, et al. Staphylococcus aureus Infects Osteoclasts and Replicates Intracellularly. *MBio.* 2019;10:e02447–19.
46. Coon D, Gulati A, Cowan C, He J. The Role of cyclooxygenase-2 (COX-2) in Inflammatory Bone Resorption. *J Endodont.* 2007;33:432–6.
47. Kang JH, Ting Z, Moon MR, Sim JS, Lee JM, Doh KE, et al. 5-Lipoxygenase Inhibitors Suppress RANKL-induced

- Osteoclast Formation via NFATc1 Expression. *Bioorg Med Chem.* 2015;23:7069–78.
48. Kubica M, Guzik K, Koziel J, Zarebski M, Richter W, Gajkowska B, et al. A potential new pathway for *Staphylococcus aureus* dissemination: the silent survival of *S. aureus* phagocytosed by human monocyte-derived macrophages. *PLoS One.* 2008;3:e1409.
 49. Smith WL, Urade Y, Jakobsson PJ. Enzymes of the cyclooxygenase pathways of prostanoid biosynthesis. *Chem Rev.* 2011;111:5821–65.
 50. Mosca M, Polentarutti N, Mangano G, Apicella C, Doni A, Mancini F, et al. Regulation of the microsomal prostaglandin E synthase-1 in polarized mononuclear phagocytes and its constitutive expression in neutrophils. *J Leukoc Biol.* 2007;82:320–6.
 51. Werner M, Jordan PM, Romp E, Czapka A, Rao Z, Kretzer C, et al. Targeting biosynthetic networks of the proinflammatory and proresolving lipid metabolome. *FASEB J.* 2019;33(5):6140–53.
 52. Murray PJ, Allen JE, Biswas SK, Fisher EA, Gilroy DW, Goerdts S, et al. Macrophage activation and polarization: nomenclature and experimental guidelines. *Immunity.* 2014;41:14–20.
 53. Pérez-Novo CA, Waeytens A, Claeys C, Van Cauwenberge P, Bachert C. *Staphylococcus aureus* Enterotoxin B Regulates Prostaglandin E2 Synthesis, Growth, and Migration in Nasal Tissue Fibroblasts. *J Infect Dis.* 2008;197:1036–43.
 54. Somayaji SN, Ritchie S, Sahraei M, Marriott I, Hudson MC. *Staphylococcus aureus* induces expression of receptor activator of NF-kappaB ligand and prostaglandin E2 in infected murine osteoblast. *Infect Immun.* 2008;76:5120–6.
 55. Wang Y, Ren B, Zhou X, Liu S, Zhou Y, Li B, et al. Growth and adherence of *Staphylococcus aureus* were enhanced through the PGE2 produced by the activated COX-2/PGE2 pathway of infected oral epithelial cells. *PLoS One.* 2017;12:e0177166.
 56. Tsai M-H, Wu C-H, Lin W-N, Cheng C-Y, Chuang C-C, Chang KT, et al. Infection with *Staphylococcus aureus* elicits COX-2/PGE2/IL-6/MMP-9-dependent aorta inflammation via the inhibition of intracellular ROS production. *Biomed Pharmacother.* 2018;107:889–900.
 57. Kalinski P. Regulation of immune responses by prostaglandin E2. *J Immunol.* 2012;188:21–8.
 58. Nakanishi M, Rosenberg DW. Multifaceted roles of PGE2 in inflammation and cancer. *Sem Immunopathol.* 2013;35:123–37.
 59. Harris SG, Padilla J, Koumas L, Ray D, Phipps RP. Prostaglandins as modulators of immunity. *Trends Immunol.* 2002;23:144–50.
 60. Sreeramkumar V, Fresno M, Cuesta N. Prostaglandin E2 and T cells: friends or foes? *Immunol Cell Biol.* 2012;90:579–86.
 61. Aronoff D, Canetti C, Peters-Golden M. Prostaglandin E2 inhibits alveolar macrophage phagocytosis through an E-prostanoid 2 receptor-mediated increase in intracellular cyclic AMP. *J Immunol.* 2004;173:559–65.
 62. Brandt SL, Klopfenstein N, Wang S, Winfree S, McCarthy BP, Territo PR, et al. Macrophage-derived LTB4 promotes abscess formation and clearance of *Staphylococcus aureus* skin infection in mice. *PLoS Pathog.* 2018;14:e1007244.
 63. Mattingly SJ, Johnston BP. Comparative analysis of the localization of lipoteichoic acid in *Streptococcus agalactiae* and *Streptococcus pyogenes*. *Infect Immun.* 1987;55:2383–6.
 64. van Langevelde P, van Dissel JT, Ravensbergen E, Appelmelk BJ, Schrijver IA, Groeneveld PH. Antibiotic-induced release of lipoteichoic acid and peptidoglycan from *Staphylococcus aureus*: quantitative measurements and biological reactivities. *Antimicrob Agents Chemother.* 1998;42:3073–8.
 65. De Kimpe SJ, Kengatharan M, Thiemermann C, Vane JR. The cell wall components peptidoglycan and lipoteichoic acid from *Staphylococcus aureus* act in synergy to cause shock and multiple organ failure. *Proc Natl Acad Sci USA.* 1995;92:10359–63.
 66. Morath S, Geyer A, Hartung T. Structure-function relationship of cytokine induction by lipoteichoic acid from *Staphylococcus aureus*. *J Exp Med.* 2001;193:393–7.
 67. Volz T, Kaesler S, Draing C, Hartung T, Röcken M, Skabytska Y, et al. Induction of IL-10-balanced immune profiles following exposure to LTA from *Staphylococcus epidermidis*. *Exp Dermatol.* 2018;27:318–26.
 68. Heim CE, Vidlak D, Kielian T. Interleukin-10 production by myeloid-derived suppressor cells contributes to bacterial persistence during *Staphylococcus aureus* orthopedic biofilm infection. *J Leukoc Biol.* 2015;98:1003–13.
 69. Sanjabi S, Zenewicz LA, Kamanaka M, Flavell RA. Anti-inflammatory and pro-inflammatory roles of TGF-beta, IL-10, and IL-22 in immunity and autoimmunity. *Curr Opin Pharmacol.* 2009;9:447–53.
 70. Gutiérrez-Venegas G, Cruz-Arrieta S, Villeda-Navarro M, Méndez-Mejía JA. Histamine promotes the expression of receptors TLR2 and TLR4 and amplifies sensitivity to lipopolysaccharide and lipoteichoic acid treatment in human gingival fibroblasts. *Cell Biol Int.* 2011;35:1009–17.
 71. Chang Y, Li P, Chen B, Chang M, Wang J, Chiu W, et al. Lipoteichoic acid-induced nitric oxide synthase expression in RAW 264.7 macrophages is mediated by cyclooxygenase-2, prostaglandin E2, protein kinase A, p38 MAPK, and nuclear factor-kappaB pathways. *Cell Signal.* 2006;18:1235–43.
 72. Yu Y, Shen Q, Lai Y, Park SY, Ou X, Lin D, et al. Anti-inflammatory Effects of Curcumin in Microglial Cells. *Front Pharmacol.* 2018;9:386.
 73. Su S, Hua K, Lee H, Chao LK, Tan S, Yang S, et al. LTA and LPS mediated activation of protein kinases in the regulation of inflammatory cytokines expression in macrophages. *Clin Chim Acta.* 2006;374:106–15.
 74. Lindner SC, Köhl U, Maier TJ, Steinhilber D, Sorg BL. TLR2 ligands augment cPLA2alpha activity and lead to enhanced leukotriene release in human monocytes. *J Leuk Biol.* 2009;86:389–99.
 75. Rutting S, Zakarya R, Bozier J, Xenaki D, Horvat JC, Wood LG, et al. Dietary Fatty Acids Amplify Inflammatory Responses to Infection through p38 MAPK Signaling. *Am J Resp Cell Mol Biol.* 2019;60:554–68.
 76. Wang X, Zhang M, Jiang N, Zhang A. Sodium Phenylbutyrate Ameliorates Inflammatory Response Induced by *Staphylococcus aureus* Lipoteichoic Acid via Suppressing TLR2/NF-kappaB/NLRP3 Pathways in MAC-T Cells. *Molecules.* 2018;23:3056.
 77. Zhao G, Jiang K, Wu H, Qiu C, Deng G, Peng X. Polydatin reduces *Staphylococcus aureus* lipoteichoic acid-induced injury by attenuating reactive oxygen species generation and TLR2-NFkappaB signalling. *J Cell Mol Med.* 2017;21:2796–808.
 78. Zhu B, Yu Y, Liu X, Han Q, Kang Y, Shi L. CD200 Modulates *S. aureus*-Induced Innate Immune Responses Through Suppressing p38 Signaling. *Int J Mol Sci.* 2019;20:659.
 79. Craig R, Larkin A, Mingo AM, Thuerauf DJ, Andrews C, McDonough PM, et al. p38 MAPK and NF-kappa B collaborate

- to induce interleukin-6 gene expression and release. Evidence for a cytoprotective autocrine signaling pathway in a cardiac myocyte model system. *J Biol Chem.* 2000;275:23814–24.
80. Kimura T, Nada S, Takegahara N, Okuno T, Nojima S, Kang S, et al. Polarization of M2 macrophages requires Lamtor1 that integrates cytokine and amino-acid signals. *Nat Commun.* 2016;7:13130.
 81. Vann JM, Proctor RA. Ingestion of *Staphylococcus aureus* by bovine endothelial cells results in time- and inoculum-dependent damage to endothelial cell monolayers. *Infect Immun.* 1987;55:2155–63.
 82. Pace S, Pergola C, Dehm F, Rossi A, Gerstmeier J, Troisi F, et al. Androgen-mediated sex bias impairs efficiency of leukotriene biosynthesis inhibitors in males. *J Clin Invest.* 2017;127:3167–76.
 83. Gründling A, Schneewind O. Synthesis of glycerol phosphate lipoteichoic acid in *Staphylococcus aureus*. *Proc Natl Acad Sci USA.* 2007;104:8478–83.

SUPPORTING INFORMATION

Additional supporting information may be found in the online version of the article at the publisher's website.

How to cite this article: Miek L, Jordan PM, Günther K, Pace S, Beyer T, Kowalak D, et al. *Staphylococcus aureus* controls eicosanoid and specialized pro-resolving mediator production via lipoteichoic acid. *Immunology.* 2022;166:47–67. <https://doi.org/10.1111/imm.13449>